Design of web-tapered steel beams against lateral-torsional buckling through a stiffness reduction method

Merih Kucukler[a,*], Leroy Gardner[b]

[a]*School of Engineering, University of Warwick, Coventry, CV4 7AL, UK*
[b]*Department of Civil and Environmental Engineering, Imperial College London, London, SW7 2AZ, UK*

Abstract

A stiffness reduction method for the lateral-torsional buckling (LTB) assessment of welded web-tapered steel beams is presented in this study. The method is implemented by (i) modelling a tapered steel beam using elastic beam finite elements specifically developed to represent the elastic instability response of tapered steel members, (ii) reducing the Young's modulus E and shear modulus G of each element through a stiffness reduction function considering the bending moments and cross-section properties at the middle of each element and (iii) performing an elastic Linear Buckling Analysis of the beam with reduced stiffness, referred to as LBA-SR herein. Since the adverse influence of the development of plasticity and imperfections on the ultimate member strengths are fully accounted for through stiffness reduction, the presented method does not require any further global instability assessment using member design equations; thus, the proposed method is both direct and practical. Verification of the method is shown for a wide range of web-tapered steel beams using results from nonlinear shell finite element modelling.

Keywords: Finite element analysis; imperfections; inelastic buckling; lateral-torsional buckling; residual stresses; stiffness reduction; structural design method; tapered beams.

1. Introduction

With the aim of optimising material use for improved economy, web-tapered steel beams are frequently utilised within steel structures. In a significant number of instances, a lateral-torsional buckling (LTB) assessment under the applied loading is required. However, the design methods provided in the current steel design specifications [1, 2] for the LTB assessment of tapered steel beams are generally mere extensions of those developed for prismatic steel beams, typically resulting in overly-conservative design and thus considerably reducing the economy gains obtained through their use.

*Corresponding author
Email addresses: merih.kucukler@warwick.ac.uk (Merih Kucukler), leroy.gardner@imperial.ac.uk (Leroy Gardner)

To address this shortcoming in the LTB assessment of tapered steel beams, alternative design methods have been put forward in the literature [3–6]. These methods are generally based on the reduction of the ultimate bending moment resistances of the cross-sections of the web-tapered beams along their lengths by means of buckling reduction factors determined using buckling curves proposed for tapered members. The influence of bending moment gradient on the development of plasticity, tapering geometry, load height, restraint type and position and the interactions between the laterally unrestrained segments during buckling on the ultimate resistances of tapered beams are typically taken into consideration through approximate and lengthy calculations within these methods [3–6], underlining the need for the development of both a practical and accurate design method for tapered steel beams.

Departing from the traditional approach of using semi-empirical member design equations, the inelastic LTB strengths of steel beams can also be determined through reducing their flexural, torsional and warping stiffnesses along their lengths considering the withstood forces and calculating their critical buckling moments, thereby accounting for the erosion of their stiffnesses due to plasticity and imperfections under the applied loading. This approach, which provides a much more direct means of determining the LTB strengths of steel members, was proposed by [7–10] for prismatic beams, though the influence of geometrical imperfections on the strengths was disregarded in these studies. The approach yet to find wide application in practice due to it being unsuitable for hand calculations. However, since structural analysis software furnishing the elastic critical buckling moments of steel members by means of Linear Buckling Analysis (LBA) is widely available nowadays, the use of stiffness reduction with LBA can now provide a very direct way of designing steel beams. Based upon this type of a design approach, Wongkaew and Chen [11] and Trahair and Hancock [12] developed stiffness reduction expressions taking into account the influence of geometrical imperfections, which were derived from the LTB curves given in the AISC load and resistance factor design specification [13] and AS 4100 [14] respectively. These proposals were however only applied to prismatic steel members. Kucukler et al. [15] developed a stiffness reduction method for the LTB assessment of steel beams, establishing its accuracy considering a broad range of cases, though again, the method was applied predominantly to only prismatic steel beams.

Extending the studies described above, a stiffness reduction approach offering a practical and accurate means of designing welded web-tapered steel beams with doubly-symmetric I sections against LTB is proposed in this paper. A stiffness reduction function able to consider fully the detrimental influence of the spread of plasticity, residual stresses and geometrical imperfections on the LTB strengths of welded beams is derived. The proposed method is applied by (i) modelling a web-tapered steel beam using elastic beam finite elements specifically developed to represent the elastic instability response of tapered members, (ii) reducing the Young's modulus E and shear modulus G of each element through the developed stiffness reduction function, thereby reducing their minor axis EI_z, warping EI_w and torsional GI_t stiffnesses and finally (iii) carrying out a Linear Buckling Analysis of the web-tapered beam with reduced stiffness, which is referred to as LBA-SR in this study. According to the presented method, the beam is assumed to have sufficient load carrying capacity only if its lowest buckling load amplifier from the LBA-SR $\alpha_{cr,op}$ is greater than or equal to unity, i.e.

$\alpha_{cr,op} \geq 1.0$, when the beam is subjected to the design loading. Owing to the ability of the stiffness reduction function to fully consider the detrimental effects of plasticity and imperfections, the presented approach does not require any further global instability assessment through semi-empirical member design equations, which can be particularly complicated for tapered steel beams, thus leading to a very practical design approach. Moreover, unlike alternative methods presented in the literature [3–6], the influence of bending moment gradient on the development of plasticity, tapering geometry, load height, restraint type and position and the interactions of laterally unrestrained segments during buckling can be directly and readily considered through the Linear Buckling Analysis with stiffness reduction (LBA-SR). In the application of the proposed method, the elastic beam finite element of Trahair [16], recently put forward to represent the elastic instability response of tapered steel members, is utilised. However, any element with the ability to accurately represent the elastic LTB response of tapered beams, such as those of [17–20], could also be employed. Thus, the presented method can be applied using any conventional structural analysis software able to provide accurate elastic critical buckling moments for tapered steel beams.

In Section 2 of this paper, shell finite element models of tapered steel beams are developed. The derivation of the stiffness reduction function for welded beams is presented in Section 3 and implementation of the stiffness reduction method is illustrated in Section 4. In the remaining sections of the paper, the accuracy of the proposed approach is demonstrated using the results from nonlinear shell finite element modelling for a wide range of web-tapered beams featuring different cross-section shapes, loading conditions and tapering geometries.

2. Finite element modelling

To verify the proposed stiffness reduction method, the results from nonlinear shell finite element modelling are utilised in this study. The finite element models were created using finite element analysis software Abaqus [21]. A reduced integration, four-noded shell element, referred to as S4R in the Abaqus [21] element library, was selected in view of its ability to provide accurate results for both thin and thick-plated steel members. 16 elements were used to model each plate constituting the flanges and web of an I section so that the spread of plasticity through the depth of the cross-section is captured accurately. To avoid overlapping of the flange and web plates, the web plate was offset considering the thickness of the flanges. 100 elements were used in the longitudinal direction for beams with length to depth ratios less than 20, whereas 200 elements were employed for larger ratios. Adopting the default Simpson integration method in the calculations, five integration points were used through the thickness of each element. The Poisson's ratio was taken as 0.3 in the elastic range and 0.5 in the plastic range by defining the effective Poisson's ratio as 0.5 so that the change of cross-sectional area under load is allowed for. The tri-linear stress-strain relationship shown in Fig. 1 was adopted as the material model, where E is the Young's modulus, E_{sh} is the strain hardening modulus, f_y and ϵ_y are yield stress and strain respectively, and ϵ_{sh} is the strain value at which strain hardening commences. The parameters f_u and ϵ_u correspond to the ultimate stress and strain values respectively. E_{sh} was assumed

to be 2% of E and ϵ_{sh} was taken as $10\epsilon_y$, conforming to the ECCS recommendations [22]. More representative values for these two parameters recently put forward by [23] will be utilised in future work. Isotropic strain hardening and the Von Mises yield criterion with the associated flow rule were employed in the finite element models. Since the constitutive formulations of Abaqus [21] adopt the Cauchy (true) stress-strain assumption for shell finite elements, the engineering stress-strain relationship shown in Fig. 1 was transformed into a true stress-strain relationship. Unless otherwise indicated, S235 steel was considered in all the simulations. Adopting the default convergence criteria recommended by Abaqus [21], the load-displacement response of the finite element models was determined by means of GMNIA (Geometrically and Materially Nonlinear Analysis with Imperfections) using the modified Riks method [24, 25].

The ECCS residual stress pattern [22] illustrated in Fig. 2, which is recommended for cross-sections fabricated through the welding of plates was applied to the finite element models. Global geometrical imperfections were assigned to the models in the form of the lowest global buckling mode, with the maximum imperfection e_0 scaled to 1/1000 of the member length as illustrated in Fig. 3; in the case of multi-span beams, the lowest global buckling mode was scaled to 1/1000 of the largest laterally unrestrained segment length. In addition to global member imperfections, local imperfections were also incorporated into the models, whose shapes were taken as the lowest local buckling modes obtained from the Linear Buckling Analyses of the shell finite element models. Following the recommendations provided in EN 1993-1-5 [26], the maximum local geometric imperfections $e_{0,loc}$ were scaled to 80% of the geometric fabrication tolerances recommended in EN 1090-2 [27] as shown in Fig. 3 (b), where h_w was conservatively taken as the largest web-depth along the length of a member. Fork end-support conditions, allowing warping deformations, were established through the use of coupling constraints at the member ends. Validation of the adopted finite element modelling approach against experimental results from the literature is provided in Kucukler [28] for a wide range of cases.

3. Development and general principles of the stiffness reduction method for the LTB assessment of web-tapered welded beams

A stiffness reduction function for the LTB assessment of welded web-tapered steel beams is presented in this section. Initially, a Perry-Robertson equation for the LTB assessment of welded prismatic steel beams under uniform bending is calibrated. Then, a stiffness reduction function derived through this Perry-Robertson equation is illustrated.

3.1. Modified Perry-Robertson equation for LTB assessment of welded beams

A stiffness reduction function for the LTB assessment of welded beams can be derived using the LTB member design equations provided in EN 1993-1-1 [1]. However, shortcomings in these equations have been identified [29, 30] and addressed through the development of an improved Perry-Robertson equation [30] that is able to represent the LTB response of prismatic beams under uniform bending more accurately. The equation of [30] was modified for the purpose of deriving a compact stiffness reduction function by Kucukler et al. [15]. In

this study, the Perry-Robertson equation modified by Kucukler et al. [15] is used to derive a stiffness reduction function for welded beams, which is given by

$$\chi_{LT} = \frac{1}{\phi_{LT} + \sqrt{\phi_{LT}^2 - \beta\overline{\lambda}_{LT}^2}} \qquad \text{where} \qquad \phi_{LT} = 0.5\left[1 + \kappa\eta_{LT} + \beta\overline{\lambda}_{LT}^2\right], \tag{1}$$

in which χ_{LT} is the buckling reduction factor to be multiplied by the plastic cross-sectional major axis bending moment resistance $M_{y,pl}$ to determine the LTB resistance of a beam $M_{b,Rd}$ with a compact (Class 1 or 2) section (i.e. $M_{b,Rd} = \chi_{LT} M_{y,pl}$), η_{LT} is a generalised imperfection factor, β is an auxiliary coefficient enabling accurate estimations of the strengths of slender beams, $\overline{\lambda}_{LT}$ is the non-dimensional LTB slenderness equal to the square root of the ratio of the plastic cross-sectional major axis bending moment resistance $M_{y,pl}$ to the elastic critical buckling moment M_{cr}, i.e. $\overline{\lambda}_{LT} = \sqrt{M_{y,pl}/M_{cr}}$. In eq. (1), κ is an auxiliary coefficient modifying the generalised imperfection factor η_{LT} by considering the degree of normal stresses resulting from the second-order minor axis and warping moments induced by the initial geometrical imperfections in a beam, which are heavily influenced by the torsional stiffness of its cross-section, thus taking into account the susceptibility of the cross-section of the beam to LTB. The auxiliary coefficient κ is determined as

$$\kappa = \frac{W_{pl,y}/A}{\frac{GI_t}{8M_{y,pl}} + \sqrt{\left(\frac{GI_t}{8M_{y,pl}}\right)^2 + I_w/I_z}}, \tag{2}$$

where G is the shear modulus, $W_{pl,y}$ is the plastic section modulus of the cross-section of the beam about the major axis, and I_w, I_t and I_z are the warping constant, torsion constant and the second moment of area about the minor axis, respectively. In Kucukler et al. [15], the Perry-Robertson equation given by eq. (1) was calibrated to the GMNIA results of hot-rolled steel beams. In the following subsection, this equation is calibrated against the ultimate strengths determined through GMNIA for welded prismatic beams under uniform bending considering a broad range of cross-section shapes and slendernesses.

3.2. Calibration of the modified Perry-Robertson equation for the LTB assessment of welded beams

Eq. (1) was calibrated by comparing the generalised imperfection factor η_{LT} against those obtained herein from finite element modelling $\eta_{LT,FE}$, adopting the procedure followed by [30]. To obtain $\eta_{LT,FE}$ values, eq. (1) was rearranged in terms of η_{LT}, resulting in the following expression:

$$\eta_{LT,FE} = \frac{1 - \chi_{LT,FE}}{\chi_{LT,FE}}\left(1 - \beta\chi_{LT,FE}\overline{\lambda}_{LT}^2\right)\frac{1}{\kappa}, \tag{3}$$

in which $\chi_{LT,FE}$ is the ratio of the ultimate strengths determined through GMNIA to the plastic bending moment capacity $M_{y,pl}$.

Employing eq. (3), eq. (1) was calibrated against the ultimate strengths determined through GMNIA considering fork-end supported welded beams subjected to uniform bending

moment. Recognising the significance of the cross-section shape on the LTB response, 20 different cross-section profiles with the same geometrical properties as those of European IPE and HE hot-rolled sections, except for the presence of the fillets, were considered. The range of the cross-sections considered is provided in Table 1, where h and b are the cross-section depth and flange width, and t_f and t_w are the flange and web thickness respectively, indicating that a large range of cross-section shapes was taken into account. For each cross-section, ten beams were analysed within the slenderness range $0.2 \leq \overline{\lambda}_{LT} \leq 2.0$, with increments in $\overline{\lambda}_{LT}$ of 0.2. Taras and Greiner [30] observed that the multiplication of η_{LT} with $\sqrt{W_{el,y}/W_{el,z}}$, where $W_{el,y}$ and $W_{el,z}$ are the elastic section moduli about the major and minor axis respectively, results in a more accurate calibration, which was adopted herein. After this enhancement and taking β as 0.6, the accuracy of the proposed generalised imperfection factor η_{LT} against those obtained from GMNIA $\eta_{LT,FE}$ is illustrated in Fig. 4 (a). As can be seen from the figure, the proposals result in high accuracy. β was taken as 0.6 since it was observed that this value results in the smallest coefficient of variation (COV) value of the ratios between η_{LT} and $\eta_{LT,FE}$. The formula proposed for the LTB assessment of steel beams is given below:

$$\chi_{LT} = \frac{1}{\phi_{LT} + \sqrt{\phi_{LT}^2 - \beta\overline{\lambda}_{LT}^2}} \qquad \text{but} \qquad \chi_{LT} \leq 1/\overline{\lambda}_{LT}^2$$
$$\text{where} \qquad \phi_{LT} = 0.5\left[1 + \kappa\alpha_{LT}\left(\overline{\lambda}_{LT} - \overline{\lambda}_{LT,0}\right) + \beta\overline{\lambda}_{LT}^2\right], \tag{4}$$

in which $\overline{\lambda}_{LT,0}$ is the plateau slenderness value below which the strength of a beam is not reduced for LTB; this value was taken as 0.2 on the basis of the GMNIA results. The calibrated values of α_{LT}, β and $\overline{\lambda}_{LT,0}$ are provided in Table 2. It was observed that specifying an upper bound for α_{LT} and a lower bound for κ increases the accuracy of eq. (4) for beams with sections highly susceptible to LTB and those less susceptible to LTB respectively. Thus, upper and lower limits were specified for α_{LT} and κ respectively, which are given in Table 2. It is worth noting that the developed LTB assessment equation given by eq. (4) is in the same form as that provided in EN 1993-1-1 [1]; thus, the values of α_{LT}, β and $\overline{\lambda}_{LT,0}$ given by [1], which are provided in Table 2, can be used in eq. (4), resulting in exactly the same LTB strength predictions as those determined through Eurocode 3 [1]. Note that Eurocode 3 [1] provides two sets of LTB assessment equations: (i) the first is given in Clause 6.3.2.2 and is applicable to beams with any cross-section shape, which will henceforth be referred to as the general case LTB assessment equation, and (ii) the second is given in Clause 6.3.2.3 and is applicable to beams with I-sections only, which will henceforth be referred to as the specific case LTB assessment equation.

The accuracy of the calibrated equation provided in eq. (4) is illustrated for prismatic welded beams with cross-section properties the same as those of HEM 340, HEA 240, HEA 500 and IPE 500 with the exception of the presence of the fillets in Fig. 4. Owing to the inclusion of the imperfection modification factor κ, the proposed LTB equation takes into account the degree of the susceptibility of the beam cross-section to LTB, leading to very accurate ultimate strength predictions for different sections and slendernesses as shown in

Fig. 4. The accuracy of the proposed LTB equation was also compared against the general and specific case LTB assessment equations provided in Eurocode 3 [1] in Table 3 for 152 beams with 20 different HE and IPE section shapes with the range of properties provided in Table 1 and different non-dimensional LTB slendernesses $\overline{\lambda}_{LT}$ ranging between 0.2 and 2.0. Note that the beams exhibiting post-buckling strengths whose resistances exceeded their elastic critical moments are not included in the table. In Table 3, N is the number of beams considered for a particular group, and S_{av}, S_{COV}, S_{max} and S_{min} are the average, coefficient of variation, maximum and minimum values of the ratios between the ultimate LTB strengths determined through the design formulae and those obtained from GMNIA respectively. As can be seen from the table, the proposed LTB assessment equation brings about considerable improvements in accuracy in comparison to the current equations provided in Eurocode 3 [1]. The ratios of the ultimate strengths of beams determined through the proposed formula and the general and specific case LTB equations $M_{y,ult,pred}$ to those obtained from GMNIA $M_{y,ult,GMNIA}$ are also illustrated in Fig. 5 for different slendernesses. As can be seen from the figure, the Eurocode 3 [1] general case LTB equation provides overly-conservative strength predictions with increasing underestimations for high slendernesses, while the Eurocode 3 [1] specific case LTB equation is quite unconservative for low-to-moderate slendernesses and conservative for high slendernesses. On the other hand, the proposed LTB equation provides results with a high level of accuracy for all the considered slenderness values.

3.3. Derivation of the stiffness reduction function for LTB assessment of welded beams

The inelastic critical buckling moment $M_{cr,i}$ of a beam can be expressed as follows

$$M_{cr,i} = \sqrt{\frac{\pi^2 (EI_z)_r}{L^2}\left[(GI_t)_r + \frac{\pi^2 (EI_w)_r}{L^2}\right]}, \tag{5}$$

where $(EI_z)_r$, $(GI_t)_r$ and $(EI_w)_r$ are the reduced minor axis, torsional and warping stiffnesses due to plasticity respectively, while L is the length of the beam. Though the reduction rates for these stiffnesses are different [10], the same reduction rate was assumed herein for the sake of simplicity in line with [15], reducing the Young's modulus E and shear modulus G through a stiffness reduction factor τ_{LT}. This enables the inelastic critical buckling moment $M_{cr,i}$ to be expressed through the multiplication of τ_{LT} with the elastic critical buckling moment M_{cr}, as shown in the equation below:

$$M_{cr,i} = \tau_{LT}\sqrt{\frac{\pi^2 (EI_z)}{L^2}\left[(GI_t) + \frac{\pi^2 (EI_w)}{L^2}\right]} = \tau_{LT} M_{cr}. \tag{6}$$

Using eq. (6), τ_{LT} can be obtained by taking the ratio of the inelastic buckling moment $M_{cr,i}$ to the elastic buckling moment M_{cr}, where the former can be determined by multiplying the plastic bending moment resistance $M_{y,pl}$ with a buckling reduction factor χ_{LT}, leading to the following expression:

$$\tau_{LT} = \frac{M_{cr,i}}{M_{cr}} = \frac{\chi_{LT} M_{y,pl}}{M_{cr}} = \chi_{LT}\overline{\lambda}_{LT}^2. \tag{7}$$

Expressing $\overline{\lambda}_{LT}$ in terms of χ_{LT} by employing the calibrated equation given by eq. (4) as described in [15] and assuming that at buckling $\chi_{LT} = M_{y,Ed}/M_{y,pl}$ (where $M_{y,Ed}$ is the applied bending moment), the following stiffness reduction function for the LTB assessment of welded steel beams is derived through eq. (7):

$$\tau_{LT} = \frac{4\psi_{LT}^2}{\kappa^2 \alpha_{LT}^2 M_{y,Ed}/M_{y,pl} \left[1 + \sqrt{1 - 4\beta\psi_{LT} \frac{M_{y,Ed}/M_{y,pl} - 1}{\kappa^2 \alpha_{LT}^2 M_{y,Ed}/M_{y,pl}}}\right]^2} \qquad \text{but} \qquad \tau_{LT} \leq 1.0$$

$$\text{where} \qquad \psi_{LT} = 1 + \overline{\lambda}_{LT,0} \kappa \alpha_{LT} \frac{M_{y,Ed}}{M_{y,pl}} - \frac{M_{y,Ed}}{M_{y,pl}}. \qquad (8)$$

The proposed values of α_{LT}, β, $\overline{\lambda}_{LT,0}$ and κ are provided in Table 2. Stiffness reduction determined through τ_{LT} under different levels of applied moment and for different cross-section shapes is shown in Fig. 6, indicating that the more susceptible the cross-section to LTB, the higher the rate of stiffness reduction. It is worth emphasising that the proposed stiffness reduction function τ_{LT} provides exactly the same LTB strength predictions as those obtained from eq. (4). Hence, its level of accuracy is the same as that shown for eq. (4) in Table 3 and Fig. 5. In lieu of the α_{LT}, β, $\overline{\lambda}_{LT,0}$ and κ values recommended in this study, those recommended in Eurocode 3 [1] for the specific and general case LTB equations, which are provided in Table 2, can also be employed within eq. (8), leading to the exactly the same strength predictions as those determined through the Eurocode 3 [1] rules, though these are less accurate than the proposals made herein. It is also worth noting that the LTB assessment equation given in eq. (4) is a modified and recalibrated version of the equation proposed by Taras and Greiner [30] for the purpose of deriving a compact stiffness reduction function τ_{LT}, as described in detail by Kucukler et al. [15], leading to ultimate strength predictions very close to those determined by the equation of [30] for both welded and hot-rolled prismatic steel beams. Thus, the compact stiffness reduction function τ_{LT} proposed herein is expected to result in ultimate strength predictions very close to those that would be determined using the stiffness reduction function derived from the LTB equation of Taras and Greiner [30].

4. Implementation of the stiffness reduction method

Application of the proposed stiffness reduction method (SRM) to welded tapered beams is illustrated in Fig. 7. As can be seen from the figure, the SRM is applied by (i) creating a beam finite element model of a tapered beam, (ii) calculating the stiffness reduction factors τ_{LT} for each beam element through eq. (8) using the bending moment values and the cross-section properties at the middle of each element, and (iii) performing an elastic Linear Buckling Analysis (LBA) of the finite element model with reduced stiffness, which will henceforth be referred to as an LBA-SR. According to the presented method, a web-tapered beam is assumed to possess sufficient load carrying capacity only if its lowest buckling load amplifier $\alpha_{cr,op}$ from the LBA-SR, which is equal to the ratio of its lowest inelastic buckling moment $M_{cr,i} = \tau_{LT} M_{cr}$ to the applied bending moment $M_{y,Ed}$, is greater than or equal to

1.0, as shown in the following expression:

$$\alpha_{cr,op} = \frac{\tau_{LT} M_{cr}}{M_{y,Ed}} \geq 1.0 \quad \text{but} \quad \tau_{LT} M_{cr} \leq M_{y,pl}. \tag{9}$$

The ultimate capacity of a beam can be determined by iterating the applied bending $M_{y,Ed}$ until reaching $\alpha_{cr,op} = 1.0$

Web-tapered steel beams with slender webs may be susceptible to local buckling effects. To capture the influence of local buckling on the LTB response of tapered beams, this study recommends the generalisation of the stiffness reduction function τ_{LT} as shown below:

$$\tau_{LT} = \frac{4\psi_{LT}^2}{\kappa^2 \alpha_{LT}^2 M_{y,Ed}/M_{y,Rd} \left[1 + \sqrt{1 - 4\beta\psi_{LT} \frac{M_{y,Ed}/M_{y,Rd} - 1}{\kappa^2 \alpha_{LT}^2 M_{y,Ed}/M_{y,Rd}}}\right]^2} \quad \text{but} \quad \tau_{LT} \leq 1.0$$

$$\text{where} \quad \psi_{LT} = 1 + 0.2\kappa\alpha_{LT} \frac{M_{y,Ed}}{M_{y,Rd}} - \frac{M_{y,Ed}}{M_{y,Rd}} \qquad \kappa = \frac{W_y/A}{\frac{GI_t}{8M_{y,Rd}} + \sqrt{\left(\frac{GI_t}{8M_{y,Rd}}\right)^2 + I_w/I_z}}, \tag{10}$$

in which W_y is the section modulus about the major axis and $M_{y,Rd}$ is the major-axis bending moment resistance equal to the multiplication of W_y with the yield stress, i.e. $M_{y,Rd} = W_y f_y$. In the application of the SRM, the compactness of the cross-section at the middle of each finite element should be considered. If the cross-section is Class 1 or 2 under bending according to EN 1993-1-1 [1], W_y should be taken as the plastic section modulus $W_{pl,y}$, whereas if the cross-section is Class 3 under bending, the recently proposed rules for the determination of the elastic-plastic major axis section modulus of Class 3 I-sections $W_{3,y}$ by Greiner et al. [31] should be adopted; this is implemented herein by using $W_{3,y}$ in eq. (10) with $M_{y,Rd} = W_{3,y} f_y$. Note though that W_y could also be conservatively taken as the elastic section modulus $W_{el,y}$ for Class 3 sections. In the case of Class 4 sections under bending, W_y should be taken as the effective section modulus $W_{y,eff}$ calculated on the basis of the rules provided in EN 1993-1-1 [1] and EN 1993-1-5 [26] with $M_{y,Rd} = W_{y,eff} f_y$. The use of smaller section moduli for Class 3 and 4 sections increases the rate of stiffness reduction (i.e. resulting in lower stiffness reduction factors τ_{LT}), thereby enabling the consideration of the influence of local instabilities on the LTB response of tapered beams.

In Kucukler et al. [15], it was shown that when a beam is subjected to transverse loading and the compression flange is not laterally restrained at the points of load application, the use of a stiffness reduction function developed through the Perry-Robertson equation for beams under uniform bending (i.e. the approach employed in the present study) can lead to overpredictions of strength since the function does not account for the additional plasticity induced by the second-order torsion from the transverse loading. In line with [15], to take into account this additional plasticity, the use of an increased imperfection factor $\alpha_{LT,F}$ equal to:

$$\alpha_{LT,F} = 1.40\alpha_{LT} \tag{11}$$

is recommended within the stiffness reduction function in this paper. Thus, when tapered beams are subjected to transverse loading and their compression flanges are not laterally

restrained at the load application points, $\alpha_{LT,F}$ should be used within eq. (10), as determined by multiplying the α_{LT} values provided in Table 2 by 1.40.

In this study, the proposed SRM is implemented utilising the elastic beam finite element developed by Trahair [16] to represent the elastic instability response of tapered steel members, which will henceforth be referred to as the 'tapered beam element' in this paper. A Matlab [32] code was written in this study based on the formulations of [16], which (i) automatically creates the finite element model of a tapered beam with the input of the geometrical and material properties and loading conditions, (ii) applies stiffness reduction to each finite element through τ_{LT} given by eq. (10), (iii) performs a Linear Buckling Analysis with stiffness reduction (LBA-SR) of the finite element model and (iv) furnishes the lowest out-of-plane buckling load factor $\alpha_{cr,op}$ of the analysed beam. For all the considered cases, the tapered beams were modelled using 10 finite elements, and the use of this number of elements is generally recommended. There exist a number of beam finite elements specifically developed to capture the elastic LTB response of tapered beams, such as those of [17–20], which can also be used in the implementation of the SRM. Thus, the proposed SRM can be applied through any structural analysis software by reducing the stiffnesses of finite elements, provided that the software is able to provide accurate elastic critical moments for tapered beams; an example of such software that is freely downloadable is [33].

In addition to the tapered beam finite elements, the use of the conventional prismatic beam elements accounting for the warping degree of freedom [34] in the application of the SRM is also investigated in this study by adopting the same described stiffness reduction procedure, where the segmented finite element models of tapered beams were created considering the cross-section properties at the middle of each element using 10 prismatic beam finite elements in all the considered cases. Note that this approach was shown to provide unreliable predictions of the elastic LTB moments of tapered beams by [18, 20, 35]. However, it was still found worthwhile to be investigated so that cases where the SRM may be applied through prismatic beam elements could be assessed.

Finally, separate checks for both shear resistance and cross-section bending moment resistance should be carried out in accordance with the provisions of EN 1993-1-1 [1] and EN 1993-1-5 [26] in the implementation of the presented method. Moreover, the proposed stiffness reduction method should be applied to tapered beams with web-tapering angles lower than or equal to 15^0, thereby excluding the cases where beam theory may not accurately represent the response.

5. Stiffness reduction method for the design of tapered beams under uniform bending moment

The presented stiffness reduction method is applied to a range of web-tapered steel beams under uniform bending with different slendernesses and tapering ratios ζ_h, equal to the ratio of the cross-section depth at the deep end h_i to that at the shallow end h (i.e. $\zeta_h = h_i/h$), in this section. Comparisons of the ultimate strength predictions determined through the presented method against those obtained from GMNIA are shown for web-tapered beams with tapering ratios ζ_h of 2.0, 3.0 and 4.0, and also for prismatic welded beams

with $\zeta_h = 1.0$, in Fig. 8. The cross-section properties at the shallow end of the investigated tapered beams were the same as those of HEM 100, HEB 360 and IPE 240 hot-rolled sections with the exception of the presence of the fillets, representing the response of beams with high, moderate and small torsional stiffness respectively. Note that in Fig. 8, $M_{y,pl,1}$ is the major axis plastic bending moment resistance of the cross-section at the shallow end, α_p is the load amplifier corresponding to the attainment of the major axis plastic bending moment resistance at the most heavily loaded cross-section, which is the cross-section at the shallow end for the considered loading condition, i.e. $\alpha_p = M_{y,pl,1}/M_{y,Ed}$, and α_{cr} is the load amplifier corresponding to elastic buckling of the considered beam, which is equal to the ratio between the elastic critical buckling moment M_{cr} and applied bending moment $M_{y,Ed}$, i.e. $\alpha_{cr} = M_{cr}/M_{y,Ed}$. The non-dimensional LTB slendernesses of the tapered steel beams were determined by taking the square root of the ratio between α_p and α_{cr}, i.e. $\overline{\lambda}_{LT} = \sqrt{\alpha_p/\alpha_{cr}}$.

Fig. 8 shows that the proposed SRM provides very accurate ultimate strength predictions of tapered steel beams with different tapering ratios ζ_h and slendernesses $\overline{\lambda}_{LT}$ when applied through the tapered beam finite elements. The tapering leads to significant enhancements in the ultimate bending moment resistance of the beams, which is very accurately captured by the proposed method. As can be seen from Fig. 8, the SRM is also accurate for the investigated beams when it is applied through the segmented finite element models created using the conventional prismatic beam finite elements, which shows that these elements provide accurate predictions of the elastic critical buckling moments M_{cr} of tapered beams under uniform bending.

In Fig. 8, the ultimate strength predictions obtained using the General Method presented in Eurocode 3 [1] for the design of nonprismatic members are also compared against those of GMNIA. According to the General Method of Eurocode 3 [1], the ultimate LTB load amplifier for a web-tapered steel beam $\alpha_{ult,GM}$ is determined by multiplying the load amplifier corresponding to the attainment of the ultimate cross-section resistance at the most heavily cross-section α_p on the basis of first-order analysis with a buckling reduction factor $\chi_{LT,GM}$, i.e. $\alpha_{ult,GM} = \chi_{LT,GM}\alpha_p$. The buckling reduction factor $\chi_{LT,GM}$ is obtained using the non-dimensional LTB slenderness $\overline{\lambda}_{LT} = \sqrt{\alpha_p/\alpha_{cr}}$ in conjunction with the buckling curves provided for the general case and specific case LTB assessment equations given in Clauses 6.2.2 and 6.2.3 of Eurocode 3 [1] respectively. The ultimate bending moment resistance of a tapered beam is reached where the ultimate LTB load amplifier is equal to 1.0, i.e. $\alpha_{ult,GM} = \chi_{LT,GM}\alpha_p = 1.0$. Adopting buckling curve 'd' (i.e. $\overline{\lambda}_{LT,0} = 0.4$ and $\alpha = 0.76$) given for the specific case LTB assessment equation to determine $\chi_{LT,GM}$, which is recommended for beams with cross-section depth h to flange width b ratios larger than 2.0, i.e. $h/b > 2.0$, the ultimate strengths obtained from Eurocode 3 are shown in Fig. 8. As can be seen from the figure, application of the General Method of Eurocode 3 [1] with the specific case buckling curve 'd' provides somewhat conservative estimations of the ultimate strengths of the beams, and also fails to capture the increased ultimate strengths with larger tapering ratios.

The accuracy of the SRM is also investigated for an additional 72 web-tapered welded steel beams with shallow end sections having the same properties as those of IPE 240, HEB 360 and HEM 100 hot-rolled sections and non-dimensional slendernesses $\overline{\lambda}_{LT}$ varying

between 0.2 and 2.0 in Table 4. In the table, N is the number of cases considered for a particular tapering ratio, and S_{av}, S_{COV}, S_{max} and S_{min} are the average, coefficient of variation, maximum and minimum of the ratios of the ultimate strengths determined through the considered design methods to those of GMNIA respectively. As can be seen from Table 4, the application of the proposed SRM in conjunction with the tapered beam elements provides accurate and safe ultimate strength predictions for a range of tapered beams under uniform bending with different tapering ratios and slendernesses. Use of conventional prismatic beam elements with the SRM also leads to accurate estimations of the ultimate strengths, though with a slightly more scatter. The accuracy of the ultimate strengths determined through the General Method of Eurocode 3 [1] using the buckling curves 'c' and 'd' given for the general and specific case LTB assesment equations, which are recommended for welded sections, is also assessed in Table 4. Note that the use of the specific and general case LTB buckling curve 'c' recommended for beams with cross-section aspect ratios h/b smaller than or equal to 2.0 could be justified for the considered tapered beams since the aspect ratios of their most heavily stressed cross-sections according to first-order analysis (i.e. those located at the shallow end) fall into this category, even though the beams feature sections with aspect ratios greater than 2.0. As can be seen from Table 4, although the use of buckling curve 'c' reduces the degree of underprediction of the strengths, Eurocode 3 [1] still yields overly-conservative results. Table 4 also shows that the general case LTB curves lead to more conservative predictions relative to the specific case LTB curves.

6. Stiffness reduction method for the design of tapered beams with varying bending moments along the length

The presented stiffness reduction method is applied to a series of welded web-tapered beams subjected to moment gradients in this section, considering tapering ratios ζ_h of 2.0, 3.0, 4.0 in addition to prismatic beams with $\zeta_h = 1.0$ and different slendernesses. The depths of web-tapered beams are usually optimised considering the varying bending moments along their lengths, thus the loading conditions considered in this section are well suited for their utilisation. Comparisons of the ultimate strength predictions determined through the presented stiffness reduction method against those obtained from GMNIA are presented in Fig. 9 for web-tapered beams with the shallow end cross-section properties the same as those of HEB 360 and IPE 240 sections with the exception of the fillets. Four end-moment ratios μ, taken as the ratio of the bending moment at the shallow end to that at the deep end, equal to 0.5, 0, -0.5 and -1 were considered (i.e. $\mu = 0.5, 0, -0.5, -1$), thus assessing the method for tapered beams under both single- and double-curvature bending. Note that $M_{y,pl,2}$ is the major axis plastic bending moment resistance of the cross-section at the deep end in Fig. 9 (b).

As can be seen from Fig. 9, the proposed SRM provides very accurate ultimate strength predictions for all the considered tapered beams subjected to different end moment ratios μ with different tapering ratios ζ_h, slendernesses $\overline{\lambda}_{LT}$ and cross-section properties. Fig. 9 (b) shows that the ultimate strengths of some beams with low slendernesses are limited by their shear strength in the case of the end-moment μ ratio of 0 (i.e.$\mu = 0$). Since the shear strength

checks are carried out according to the provisions of Eurocode 3 [1] in the application of the presented method, the beneficial influence of strain hardening is neglected, unlike in the GMNIA performed herein. Thus, the ultimate strength predictions obtained for these beams are quite conservative. Fig. 9 also shows that the use of conventional prismatic beam elements with the SRM also leads to the accurate estimations of the strengths, which can again be attributed to their accuracy in the prediction of the elastic critical bending moments of the investigated fork-end supported singly-tapered beams. It can also be seen from Fig. 9 that the SRM provides accurate predictions of the ultimate resistances of stocky tapered steel beams when the ultimate capacity is dominated by cross-section bending moment resistances but the influence of instability effects is still present, i.e. when $\tau_{LT}M_{cr}$ is close to M_{pl} but $\tau_{LT}M_{cr} < M_{pl}$. The accuracy of the SRM for similar cases was also verified in Kucukler et al [15].

In addition to tapered beams with varying end moments, the accuracy of the proposed SRM was also investigated for those subjected to a point load at the mid-span of the beam. Comparisons of the ultimate strengths determined through the SRM against the GMNIA results are provided in Fig. 10 for tapered beams subjected to a point load at the mid-span with four tapering ratios $\zeta_h = 1.0, 2.0, 3.0, 4.0$ and cross-section properties the same as those of HEM 100 and HEB 360 at the shallow ends. In Fig. 10, $M_{y,pl,mid}$ is the plastic bending moment resistance of the cross-sections at the mid-span of the tapered beams. Note that in all the considered cases, the point load was applied at the shear centre of the section. As described in Section 4, the increased imperfection factor $\alpha_{LT,F}$ equal to $\alpha_{LT,F} = 1.40\alpha_{LT}$ was considered in the determination of the stiffness reduction factors τ_{LT} since lateral restraints were not provided to the compression flanges at the load application points. Fig. 10 shows that the proposed SRM leads to very accurate estimations of the ultimate strengths of tapered beams subjected to transverse loading. Similarly to the previous cases, application of the SRM through both tapered and prismatic beam elements lead to high accuracy. The ultimate strength predictions of the tapered beams determined through the General Method of Eurocode 3 [1] with the specific case LTB curve 'd' are also shown in Fig. 10. As can be seen from the figure, Eurocode 3 provides much less accurate results than the SRM, significantly overpredicting the ultimate strengths of tapered beams with the HEB 360 section at the shallow end and large tapering ratios (i.e. $\zeta_h = 3.0, 4.0$).

In addition to the considered tapered beams, the accuracy of the proposed SRM is also assessed against GMNIA results for 334 web-tapered steel beams subjected to different loading conditions with the section shapes having the properties the same as those of IPE 240, HEB 360 and HEM 100 with the exception of the presence of fillets at the shallow ends in Table 5. In the table, three tapering ratios ζ_h equal to 2.0, 3.0 and 4.0 and non-dimensional slendernesses ranging between 0.4 and 2.0 are considered for each loading condition. Note that the beams exhibiting significant post-buckling strengths (i.e. the beams whose ultimate resistances exceeded their elastic buckling moments, though with large accompanying deformations), those whose ultimate resistances exceeded the plastic bending moment resistances of their most heavily loaded sections due to strain hardening and those undergoing shear failure were not considered in the table. As can be seen from Table 5, the proposed SRM provides very accurate ultimate strength predictions for the wide range of considered cases

with S_{av} values equal to or very close to 1.0 with small coefficient of variation S_{COV} values, verifying the accuracy of the method. The use of both tapered and prismatic beam elements leads to high accuracy, though the use of the former is always recommended. The accuracy of Eurocode 3 [1] is also assessed for all the considered beams in Table 5. Note that the buckling curves determined considering the aspect ratios h/b of the most heavily stressed cross-sections according to the applied first-order moments are used in the application of the General Method of Eurocode 3. It can be seen from Table 5 that Eurocode 3 [1] provides results that are generally on the safe side, but rather scattered, as well as some quite unconservative strength predictions. These results on the unsafe side were generally observed for beams under single-curvature bending with more uniform stresses along their lengths, i.e. those subjected to bending moments varying in accordance with their section depths and those subjected to transverse loading which is also illustrated in Fig. 10 (b).

7. Stiffness reduction method for the design of doubly-tapered, multi-span and cantilever tapered beams

The accuracy of the proposed SRM is investigated for doubly-tapered beams, tapered beams with elastic restraints, multi-span braced tapered beams and cantilever tapered beams in this section.

7.1. Doubly-tapered beams

In this subsection, the SRM is applied to the doubly-tapered beams investigated by Yang and Yau [36], which were also analysed by Andrade and Camotim [20]. The reference investigated beam, subjected to a point load at the shear centre of the mid-span section, has a length L of 6.096 m and a cross-section at the mid-span whose depth h_i, flange width b, flange and web thicknesses t_f and t_w are equal to 609.6 mm, 152.4 mm, 12.7 mm and 9.5 mm respectively. Using this cross-section shape at the mid-span, different tapering ratios ζ_h were considered by modifying the cross-section depths at the ends h, i.e. $1/\zeta_h = h/h_i$. In addition to the beams with a length of 6.096 m originally investigated by [20, 36], beams with a length of 3.048 m and the same cross-section shape at the mid-span are also investigated herein. The ultimate strength predictions determined through the SRM are compared against those of GMNIA in Fig. 11 (a), where $M_{y,pl,middle}$ is the major axis plastic bending moment resistance of the mid-span section. As can be seen from the figure, the SRM provides accurate and safe estimations of ultimate strengths when applied through the tapered beam elements. The strength of a beam with a length of 3.048 m and a tapering ratio equal to $1/\zeta_h = 0.2$ is overestimated. However, the web tapering angle is larger than 15^{O} for this beam, thus it is outside of the range where the SRM is applicable. Unlike when it is used with the tapered beam finite elements, the SRM overpredicts the ultimate strengths of the doubly-tapered beams in the cases where it is applied through the prismatic beam finite elements as can be seen from Fig. 11 (a). This results from the overpredictions of the elastic critical buckling moments by the prismatic beams elements as shown in Fig. 11 (b), where the elastic critical moments determined through the tapered and prismatic beam elements models are compared against those obtained from shell element models for all the considered beams. It can be

seen from the figure that unlike tapered beam finite element models, the elastic buckling moments are overpredicted when prismatic beam element models are used, which is in line with the observations of [20, 36]. The overpedictions are particularly high for the shorter beams ($L = 3.048$ m), increasing with the larger web tapering angles. These unconservative estimations of the elastic critical bending moments may be attributed to the inability of the prismatic beam elements to account for the second-order torsional moments $T_{w\perp}$ arising in web-tapered beams, which result from the vertical components $\sigma_{w\perp}$ of the warping normal stresses σ_w developing within the inclined flanges as shown in Fig. 12. Consideration of this influence is of particular importance for doubly-tapered beams when the warping stressses assume their greatest values within the vicinity of the mid-span where torsional restraints are not provided, as shown in Fig. 13; this is unlike the majority of the singly-tapered beams considered in the previous sections. This behaviour and other shortcomings of analysing tapered members with the prismatic beam elements have also been discussed by [20, 37, 38].

In Fig. 14, the ultimate strengths determined through the SRM are compared against those of GMNIA for doubly-tapered beams subjected to uniform bending with a cross-section shape having the properties the same as those of IPE 240 at the shallow ends and with different slendernesses $\overline{\lambda}_{LT}$ and tapering ratios ζ_h. Similar to the Yang and Yau [36] beams, the SRM provides accurate and safe ultimate strength predictions for all the considered tapering ratios and slendernesses with the tapered beam elements, while the use of the prismatic beam elements leads to significant overpredictions of the strengths. Based on the observations made in this subsection, the use of only tapered beam finite elements is recommended in the application of the SRM to doubly-tapered beams.

7.2. Doubly-tapered beam with elastic lateral restraint

In this subsection, the application of the stiffness reduction method to a doubly-tapered steel beam with an elastic restraint and subjected to a point load at the midspan is investigated. The non-dimensional LTB slenderness $\overline{\lambda}_{LT} = \sqrt{\alpha_p/\alpha_{cr}} = \sqrt{1/(M_{cr}/M_{y,pl,mid})}$ of the considered beam, whose section at the shallow ends have the same properties as those of a hot-rolled HEB 360 section without fillets, is equal to 1.0. The elastic lateral restraint was applied to the compression flange at the mid-span where the point load was acting at the shear centre. The stiffness of the lateral-restraint K was varied and the ultimate strengths of the doubly-tapered beam were determined through the SRM, GMNIA and the General Method of Eurocode 3 using the specific case LTB curve 'd' since the aspect ratio h/b of the most stressed section is larger than 2.0. Two types of geometrical imperfection were taken into account in the implementation of the GMNIA: one-half sine wave and two-half sine waves utilising the first and second buckling modes of the doubly-tapered beam. A comparison of the ultimate strength predictions determined through the SRM, GMNIA and Eurocode 3 are provided in Fig. 15, in which K_L is the elastic threshold restraint stiffness resulting in the elastic buckling of the beam in the second mode. Fig. 15 illustrates that up to a specific stiffness value $K_{L,inelastic}$, GMNIA with the geometrical imperfection in the form of the first buckling mode results in lower strength predictions relative to those determined with the imperfection in the form of the second buckling mode. For larger restraint stiffness, GMNIA with the two-half sine wave imperfection shape leads to lower strengths. This spe-

cific stiffness value can be referred to as the inelastic threshold stiffness $K_{L,inelastic}$, resulting in the inelastic buckling of the doubly-tapered beam in the second buckling mode. The development of plasticity within the beam increases the relative effectiveness of the support afforded by the elastic restraint since the ratio of the restraint stiffness to the beam stiffness becomes greater. Hence, the inelastic threshold stiffness $K_{L,inelastic}$ is significantly smaller than the elastic threshold stiffness K_L. Fig. 15 shows that the proposed SRM is capable of considering this increased effectiveness of the elastic restraint. As mentioned, this study recommends the use of the increased imperfection factor $\alpha_{LT,F} = 1.40\alpha_{LT}$ in the stiffness reduction function τ_{LT} in the cases where lateral restraints are not provided to the compression flanges at the load application points. The compression flange of the beam is laterally restrained at the load application point in this case, though the lateral restraint is not rigid. Thus, the SRM is applied using both $\alpha_{LT,F}$ and α_{LT} herein. The SRM with the increased imperfection factor $\alpha_{LT,F}$ provides accurate strength estimations up to the proximity of the inelastic threshold stiffness, after which the SRM with the unmodified imperfection factor α_{LT} leads to slightly more accurate estimations; the latter is unconservative for K values less than $K_{L,inelastic}$ though. On the basis of these observations, this study recommends the use the increased imperfection factor $\alpha_{LT,F}$ up to the elastic threshold stiffness value K_L for tapered beams with elastic lateral restraints since it only provides slight underpredictions of the strengths after the inelastic threshold stiffness $K_{L,inelastic}$ is exceeded. As can be seen in Fig. 15, unlike the SRM, Eurocode 3 [1] fails to capture the increased effectiveness of the lateral restraint and leads to overly conservative predictions for the considered lateral stiffness values.

7.3. Braced tapered beams

In this subsection, the proposed SRM is applied to a series of tapered beams braced at two intermediate points along the span whose end sections have the same properties of an HEM 100 section. As can be seen from Fig. 16, two different values of outer segment L_o to inner segment L_i ratios are considered: 0.5 and 2.0 (i.e. $L_o/L_i = 0.5, 2.0$). According to the elastic buckling analyses of the beams, which exhibit interaction between the unbraced beam lengths [39], the inner segments are critical for beams with $L_o/L_i = 0.5$, while the outer segments are critical for those with $L_o/L_i = 2.0$. Since the lateral restraints are provided to the compression flanges at the load application points, the unmodified imperfection factor α_{LT} was used in the application of the SRM. The ultimate strengths determined through the SRM, GMNIA and the General Method of Eurocode 3 [1] are compared for different slenderness values $\overline{\lambda}_{LT}$ and tapering ratios ζ_h of 1,0, 2.0 and 4.0 in Fig. 16, where $M_{y,pl,2}$ is the major axis plastic bending moment resistance of the deepest cross-section of the beam (i.e. the cross-section at the middle segment). As can be seen from the figure, the SRM provides very accurate ultimate strength predictions for the multi-braced tapered beams when it is applied by means of either tapered or prismatic finite elements. The ultimate strengths of the tapered beams are accurately predicted in the cases where the inner or outer segments are critical. Moreover, the interactive inelastic buckling of the multi-braced tapered beams are directly and practically captured through the Linear Buckling Analysis with stiffness reduction (i.e. LBA-SR). Fig. 16 shows that prismatic beams (i.e. those with

$\zeta_h = 1.0$) exhibit some post-buckling strength for high slendernesses but this is not of practical relevance as the span-to-depth ratios of these beams are outside the range likely to be used in practice. As can be seen from Fig. 16, the General Method of Eurocode 3 [1] provides significantly overly-conservative ultimate strength predictions for the braced tapered beams and the proposed SRM leads to considerably more accurate ultimate strength predictions.

7.4. Cantilever tapered beams

The response of cantilever beams is very different to that of beams supported at the both ends as described by Trahair [40]. In this subsection, the proposed SRM is applied to a range of tapered cantilever beams whose cross-section at the shallow end have the same properties of an HEB 360 section without fillets. Note that the beams were subjected to point loads applied to the shear centre at the free shallow ends. Since no lateral restraint is provided at the load application points, the SRM was applied with the increased imperfection factor $\alpha_{LT,F} = 1.40\alpha_{LT}$. The ultimate strengths determined through the SRM are compared against those determined through GMNIA and Eurocode 3 in Fig. 17 (a) for different tapering ratios. As can be seen from the figure, the SRM provides quite conservative ultimate strength predictions. This is not surprising since its stiffness reduction function τ_{LT} provided by eq. (8) was developed considering the response of beams supported at the both ends. On the other hand, the use of the unmodified imperfection factor α_{LT} in the determination of the stiffness reduction factor leads to more accurate ultimate strength predictions as can be seen from Fig. 17 (b). Fig. 17 also shows that Eurocode 3 [1] leads to overly-conservative strength predictions for the cantilever tapered beams. Based on the observations made in this subsection, the use of the unmodified imperfection factor α_{LT} is recommended in the application of the SRM to cantilever tapered beams. Future research will focus on simple modifications to the developed stiffness reduction function τ_{LT} given by eq. (10) so as to achieve more accurate strength predictions for cantilever tapered beams.

8. Conclusions

In this paper, a stiffness reduction method (SRM) for the lateral-torsional buckling (LTB) assessment of welded web-tapered steel beams featuring doubly-symmetric cross-sections is proposed. The presented method is applied by reducing the Young's modulus E and shear modulus G of a tapered beam by means of a stiffness reduction function and performing an elastic Linear Buckling Analysis with reduced stiffness, referred to as an LBA-SR in this study. Considering the need of scope for improvement to the LTB assessment equations provided in Eurocode 3 [1], a Perry-Robertson LTB assessment equation in the same form as those recommended in [1] was calibrated considering a wide range of prismatic welded beams subjected to uniform bending and with 20 different section shapes with the same properties of European IPE and HE sections with the exception of the fillets. Utilising the GMNIA results of 152 welded beams subjected to uniform bending, significantly higher level of accuracy brought about by the calibrated Perry-Robertson equation in comparison to Eurocode 3

[1] was illustrated. A stiffness reduction function was derived using the calibrated Perry-Robertson equation, resulting in the same ultimate strength predictions as those determined through this equation for prismatic welded beams under uniform bending. Following the derivation of the stiffness reduction function, the accuracy of the proposed SRM was verified for 72 tapered beams under uniform bending with different tapering ratios, section shapes and slendernesses. The accuracy of the proposed SRM was also assessed against GMNIA results for 334 tapered beams subjected to various bending moment shapes and featuring various tapering ratios, section shapes and slendernesses. It was shown that the presented SRM leads to very accurate and safe estimations of ultimate strengths of tapered beams. In addition to a large number of singly-tapered beams, the accuracy of the proposed SRM has also been illustrated for doubly-tapered beams, tapered beams with an elastic restraint, laterally braced tapered beams featuring interactive buckling of the unbraced segments and cantilever tapered beams. The accuracy of using beam finite elements specifically developed to represent the elastic instability response of tapered steel members versus conventional prismatic beam elements in conjunction with the proposed SRM was also investigated. It was shown that even though the conventional prismatic beam elements lead to accurate results for singly-tapered beams, they provide significant overestimations of the ultimate strengths for doubly-tapered beams, while the tapered beam finite elements furnished accurate results in all the considered cases. Thus, their use is recommended in the application of the proposed method.

The presented stiffness reduction method offers a very practical means of determining the LTB strengths of web-tapered steel beams. Unlike alternative methods proposed for the design of tapered beams in the literature, it enables the consideration of the influence of moment gradient, load height, restraint type (e.g. elastic, rigid, translational or rotational) and position, and interactions of laterally unrestrained segments during buckling on the ultimate resistances through the LBA-SR in a very direct way. The proposed method can be applied by means of any conventional structural analysis software that can accurately determine elastic buckling moments of tapered steel beams. The practicality and accuracy of using LBA in conjunction with stiffness reduction has also been shown by [41]. It is worth noting that web-tapered steel beams can undergo distortional failure modes in some cases as indicated by Ronagh and Bradford [42]. Based on the geometries considered in this study, it is recommended to limit the maximum web height h_w to web thickness t_w ratios to 120 within tapered beams, i.e. $h_w/t_w \leq 120$, in the application of the proposed SRM. Future research will focus on the extension of the proposed method to the flexural-torsonal buckling assessment of tapered beam-columns following the recommendations of [43] and considering the influence of pre-buckling effects [44–46], and on the instability assessment of tapered members featuring monosymmetric cross-sections.

References

[1] EN 1993-1-1, Eurocode 3 Design of steel structures-Part 1-1: General rules and rules for buildings. European Committee for Standardization (CEN), Brussels; 2005.

[2] AISC 360-10, Specifications for structural steel buildings. American Institute of Steel Construction (AISC), Chicago; 2010.

[3] Shiomi, H., Kurata, M.. Strength formula for tapered beam-columns. Journal of Structural Engineering, ASCE 1984;110(7):1630–1643.
[4] Braham, M., Hanikenne, D.. Lateral buckling of web tapered beams: An original design method confronted with a computer simulation. Journal of Constructional Steel Research 1993;27(1):23–36.
[5] Polyzois, D., Raftoyiannis, I.G.. Lateral-torsional stability of steel web-tapered I-beams. Journal of Structural Engineering, ASCE 1998;124(10):1208–1216.
[6] Marques, L., da Silva, L.S., Greiner, R., Rebelo, C., Taras, A.. Development of a consistent design procedure for lateral–torsional buckling of tapered beams. Journal of Constructional Steel Research 2013;89:213–235.
[7] Neal, B.G.. The lateral instability of yielded mild steel beams of rectangular cross-section. Philosophical Transactions of the Royal Society of London A: Mathematical, Physical and Engineering Sciences 1950;242(846):197–242.
[8] Wittrick, W.H.. Lateral instability of rectangular beams of strain-hardening material under uniform bending. Journal of the Aeronautical Sciences 1952;19(12).
[9] Galambos, T.V.. Inelastic lateral buckling of beams. Journal of the Structural Division, ASCE 1963;89(5).
[10] Trahair, N.S., Kitipornchai, S.. Buckling of inelastic I-beams under uniform moment. Journal of the Structural Division, ASCE 1972;98(11).
[11] Wongkaew, K., Chen, W.F.. Consideration of out-of-plane buckling in advanced analysis for planar steel frame design. Journal of Constructional Steel Research 2002;58(5):943–965.
[12] Trahair, N.S., Hancock, G.J.. Steel member strength by inelastic lateral buckling. Journal of Structural Engineering, ASCE 2004;130(1):64–69.
[13] AISC-LRFD, Load and resistance factor design specification for structural steel buildings. AISC, Chicago; 1993.
[14] Standards Australia, AS 4100 steel structures. Australian Building Codes Board, Sydney; 1998.
[15] Kucukler, M., Gardner, L., Macorini, L.. Lateral–torsional buckling assessment of steel beams through a stiffness reduction method. Journal of Constructional Steel Research 2015;109:87–100.
[16] Trahair, N.. Lateral buckling of tapered members. Engineering Structures 2017;151:518–526.
[17] Bradford, M.A., Cuk, P.E.. Elastic buckling of tapered monosymmetric I-beams. Journal of Structural Engineering, ASCE 1988;114(5):977–996.
[18] Ronagh, H., Bradford, M., Attard, M.. Nonlinear analysis of thin-walled members of variable cross-section. Part I: Theory. Computers & Structures 2000;77(3):285–299.
[19] Boissonnade, N., Muzeau, J.. A new beam finite element for tapered members. In: Proceedings of the eighth international conference on the application of artificial intelligence to civil and structural engineering computing. Civil-Comp Press; 2001, p. 73–74.
[20] Andrade, A., Camotim, D.. Lateral–torsional buckling of singly symmetric tapered beams: theory and applications. Journal of Engineering Mechanics, ASCE 2005;131(6):586–597.
[21] Abaqus v.6.14 Reference Manual. Simulia, Dassault Systemes; 2014.
[22] ECCS, Ultimate limit state calculation of sway frames with rigid joints. Tech. Rep.; No. 33, Technical Committee 8 (TC 8) of European Convention for Constructional Steelwork (ECCS); 1984.
[23] Yun, X., Gardner, L.. Stress-strain curves for hot-rolled steels. Journal of Constructional Steel Research 2017;133:36–46.
[24] Crisfield, M.A.. A fast incremental/iterative solution procedure that handles "snap-through". Computers & Structures 1981;13(1-3):55–62.
[25] Ramm, E.. Strategies for tracing the nonlinear response near limit points. In: Nonlinear finite element analysis in structural mechanics. Springer; 1981, p. 63–89.
[26] EN 1993-1-5, Eurocode 3 Design of steel structures-Part 1-5: Plated structural elements. European Committee for Standardization (CEN), Brussels; 2005.
[27] EN 1990-2, Execution of Steel Structures and Aluminium Structures-Part 2: Technical Requirements for Steel Structures. European Committee for Standardization (CEN), Brussels; 2008.
[28] Kucukler, M.. Stiffness reduction approach for structural steel design. Ph.D. thesis; Imperial College

London; 2015.
[29] Rebelo, C., Lopes, N., da Silva, L.S., Nethercot, D., Real, P.V.. Statistical evaluation of the lateral–torsional buckling resistance of steel I-beams, Part 1: Variability of the Eurocode 3 resistance model. Journal of Constructional Steel Research 2009;65(4):818–831.
[30] Taras, A., Greiner, R.. New design curves for lateral–torsional buckling -— Proposal based on a consistent derivation. Journal of Constructional Steel Research 2010;66(5):648–663.
[31] Greiner, R., Kettler, M., Lechner, A., Jaspart, J., Boissonade, N., Bortolotti, E., et al. SEMI-COMP: Plastic Member Capacity of Semi-Compact Steel Sections–a more Economic Design: Final Report. Research Fund for Coal and Steel, European Commission; 2009.
[32] Matlab version 8.5.0 (R2015a). Mathworks Inc.; 2015.
[33] LTBeamN v.1.0.1. Lateral-torsional buckling of beam-columns. CTICM, https://www.cticm.com/content/ltbeamn-logiciel-deversement-elastique-poutres (Accessed: 2018-10-05); 2018.
[34] Barsoum, R.S., Gallagher, R.H.. Finite element analysis of torsional and torsional–flexural stability problems. International Journal for Numerical Methods in Engineering 1970;2(3):335–352.
[35] Jeong, W.Y.. Structural analysis and optimized design of general nonprismatic I-section members. Ph.D. thesis; Georgia Institute of Technology; 2014.
[36] Yang, Y.B., Yau, J.D.. Stability of beams with tapered I-sections. Journal of Engineering Mechanics, ASCE 1987;113(9):1337–1357.
[37] Andrade, A., Camotim, D., Dinis, P.B.. Lateral-torsional buckling of singly symmetric web-tapered thin-walled i-beams: 1d model vs. shell fea. Computers & Structures 2007;85(17-18):1343–1359.
[38] Bradford, M.. Stability of tapered i-beams. Journal of Constructional Steel Research 1988;9(3):195–216.
[39] Trahair, N.S.. Interaction buckling of tapered beams. Engineering Structures 2014;62:174–180.
[40] Trahair, N.S.. Flexural-torsional buckling of structures; vol. 6. CRC Press; 1993.
[41] Subramanian, L., White, D.W.. Reassessment of the lateral torsional buckling resistance of rolled I-section members: Moment gradient tests. Journal of Structural Engineering, ASCE 2016;143(4):04016203.
[42] Ronagh, H.R., Bradford, M.A.. Parameters affecting distortional buckling of tapered steel members. Journal of Structural Engineering, ASCE 1994;120(11):3137–3155.
[43] Kucukler, M., Gardner, L., Macorini, L.. Flexural–torsional buckling assessment of steel beam–columns through a stiffness reduction method. Engineering Structures 2015;101:662–676.
[44] Kucukler, M., Gardner, L.. Design of laterally-restrained web-tapered steel structures through a stiffness reduction method. Journal of Constructional Steel Research 2018;141:63–76.
[45] Kucukler, M., Gardner, L., Macorini, L.. A stiffness reduction method for the in-plane design of structural steel elements. Engineering Structures 2014;73:72–84.
[46] Kucukler, M., Gardner, L., Macorini, L.. Development and assessment of a practical stiffness reduction method for the in-plane design of steel frames. Journal of Constructional Steel Research 2016;126:187–200.

Figures captions

Figure 1 : Material stress-strain curved used in finite element simulations

Figure 2 : Residual stress pattern applied to finite element simulations (+ve tension, -ve compression)

Figure 3 : Incorporation of geometrical imperfections into finite element models using global and local buckling modes

Figure 4 : Calibration of the proposed Perry-Robertson equation and assessment of its accuracy against GMNIA results for beams with different cross-section shapes

Figure 5 : Stiffness reduction for different welded cross-section shapes

Figure 6 : Stiffness reduction for different welded cross-section shapes

Figure 7 : Application of the proposed stiffness reduction method (SRM) to web-tapered steel beams

Figure 8 : Accuracy of the proposed stiffness reduction method (SRM) in comparison to shell finite element GMNIA and Eurocode 3 [1] for tapered beams under uniform bending with different section shapes and slendernesses

Figure 9 : Accuracy of the proposed stiffness reduction method (SRM) in comparison to shell finite element GMNIA for tapered beams under moment gradient with different section shapes and slendernesses

Figure 10 : Accuracy of the proposed stiffness reduction method (SRM) in comparison to shell finite element GMNIA and Eurocode 3 [1] for tapered beams subjected to a point load at mid-span with different section shapes and slendernesses

Figure 11 : Accuracy of the stiffness reduction method (SRM) when applied using tapered or prismatic elastic finite elements and accuracy of tapered and prismatic element models in predicting the elastic critical buckling moments of doubly tapered beams ($h_i = 609.6$ mm, $b = 152.4$ mm, $t_w = 9.5$ mm, $t_f = 12.7$ mm)

Figure 12 : Development of second-order torque $T_{w\perp}$ due to the vertical component $\sigma_{w\perp}$ of the warping normal stresses within flanges σ_w

Figure 13 : Finite element model of the doubly-tapered Yang and Yau [36] steel beam with $L = 6096$ mm and $1/\zeta_h = 0.2$ after failure

Figure 14 : Accuracy of the proposed stiffness reduction method (SRM) in comparison to shell finite element GMNIA for doubly-tapered beams

Figure 15 : Comparison of ultimate strength predictions determined through the proposed stiffness reduction method (SRM) against shell finite element GMNIA and Eurocode 3 for doubly tapered beams with elastic lateral restraint

Figure 16 : Comparison of ultimate strength predictions determined through the proposed stiffness reduction method (SRM) against shell finite element GMNIA and Eurocode 3 for braced tapered beams

Figure 17 : Comparison of ultimate strength predictions determined through the proposed stiffness reduction method (SRM) against shell finite element GMNIA and Eurocode 3 for cantilever tapered beams

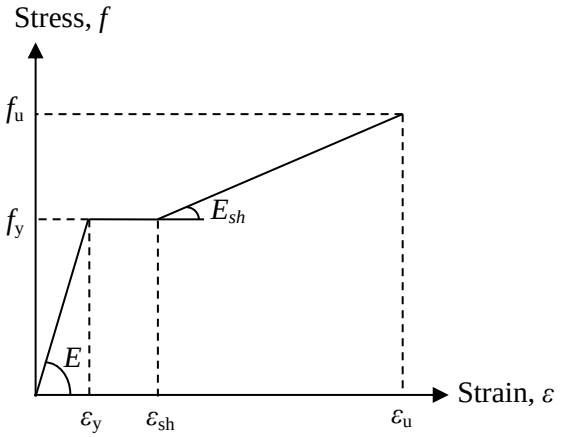


Figure 1: Material stress-strain curved used in finite element simulations

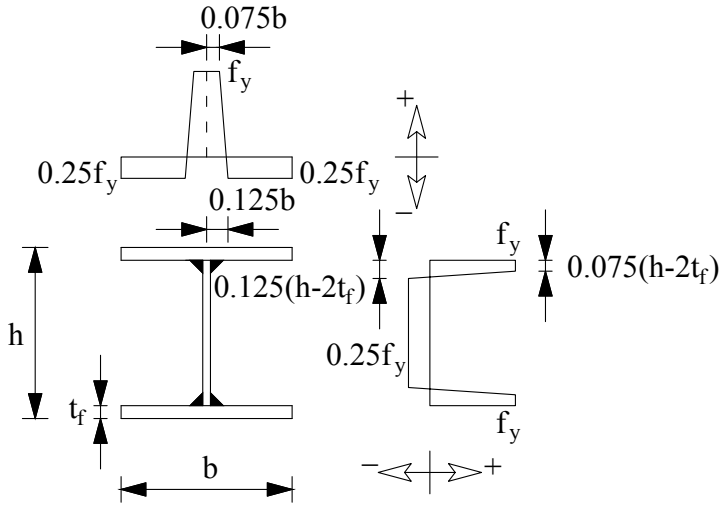
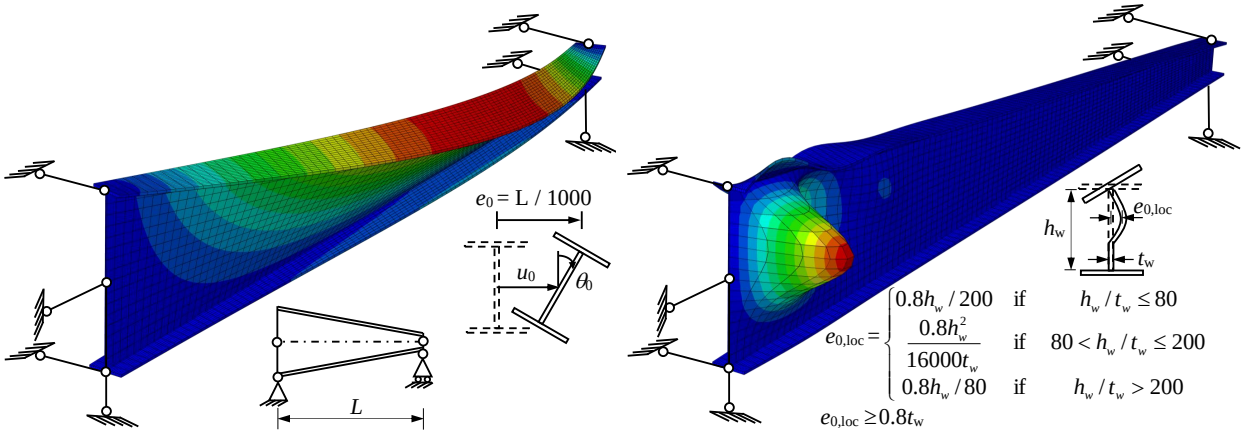
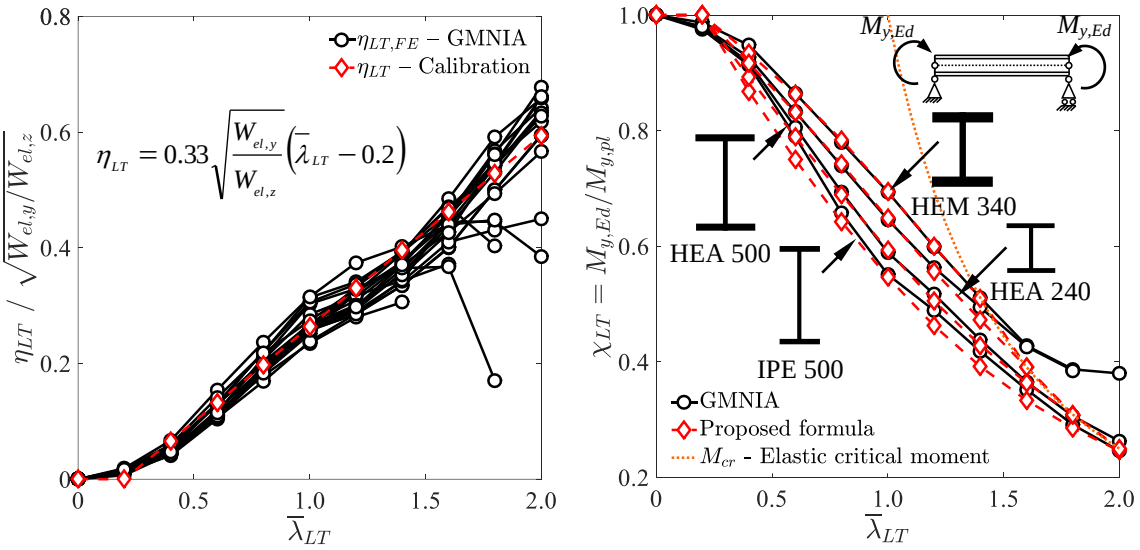


Figure 2: Residual stress pattern applied to finite element simulations (+ve tension, -ve compression)



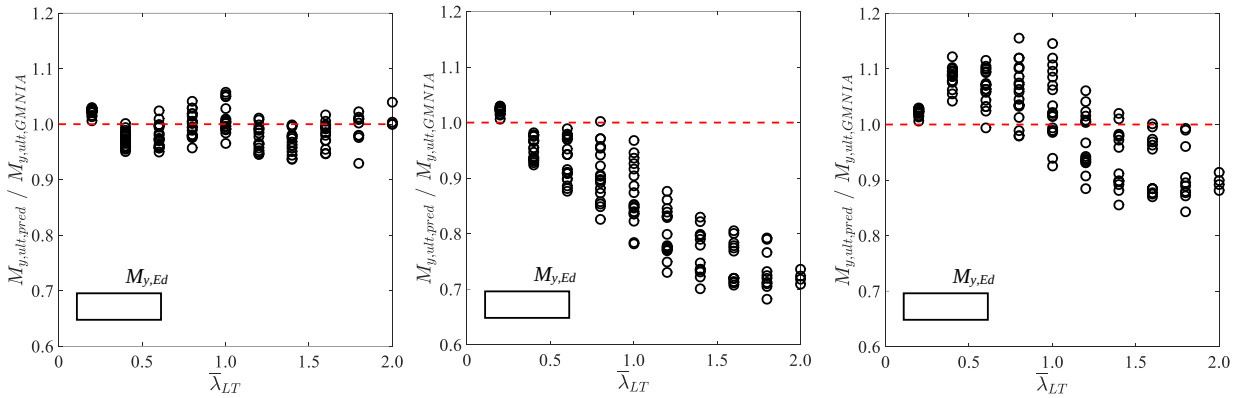
(a) Global geometrical imperfections (b) Local geometrical imperfections

Figure 3: Incorporation of geometrical imperfections into finite element models using global and local buckling modes



(a) Calibration (b) Accuracy of the formula

Figure 4: Calibration of the proposed Perry-Robertson equation and assessment of its accuracy against GMNIA results for beams with different cross-section shapes



(a) Proposed equation (b) EC3 General (c) EC3 Specific

Figure 5: Comparison of the accuracy of the ultimate strength predictions obtained from the proposed Perry-Robertson equation and the Eurocode 3 [1] general and specific case LTB assessment equations

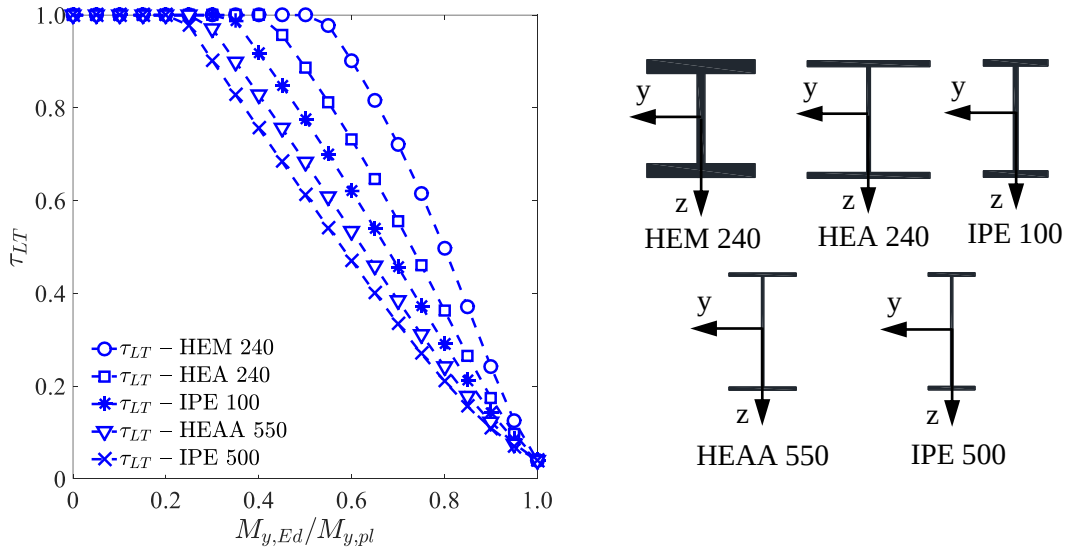
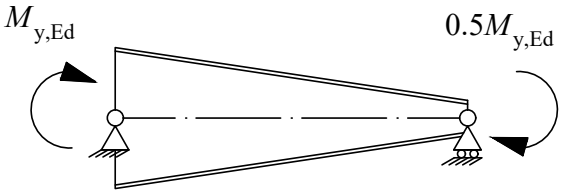
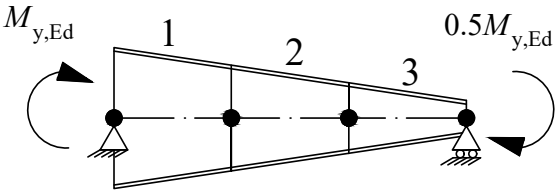


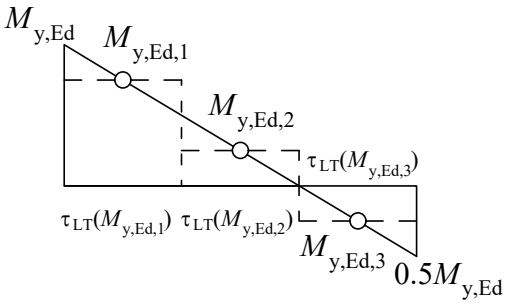
Figure 6: Stiffness reduction for different welded cross-section shapes



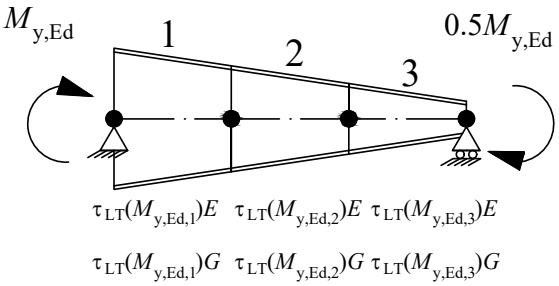
(a) Web-tapered beam to be designed



(b) Step 1: Create finite element model of beam using elastic tapered beam elements

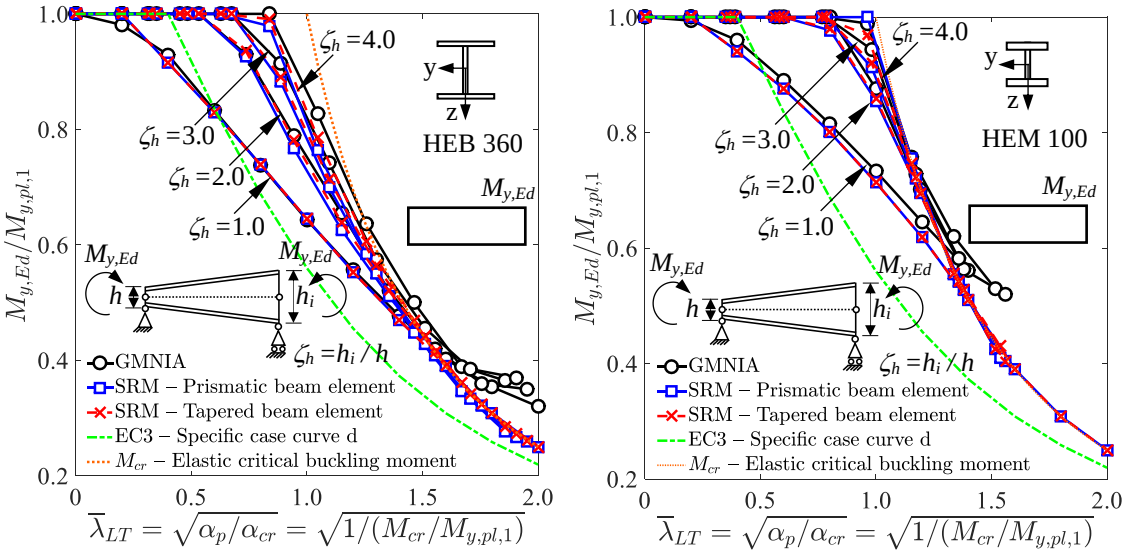


(c) Step 2: Determine stiffness reduction factors τ_{LT} for each finite element using bending moment values and cross-section properties at the middle of each element



(d) Step 3: Reduce the Young's E and shear G moduli of each element using corresponding τ_{LT} values, perform Linear Buckling Analysis (LBA-SR) and check $\alpha_{cr,op} \geq 1.0$

Figure 7: Application of the proposed stiffness reduction method (SRM) to web-tapered steel beams

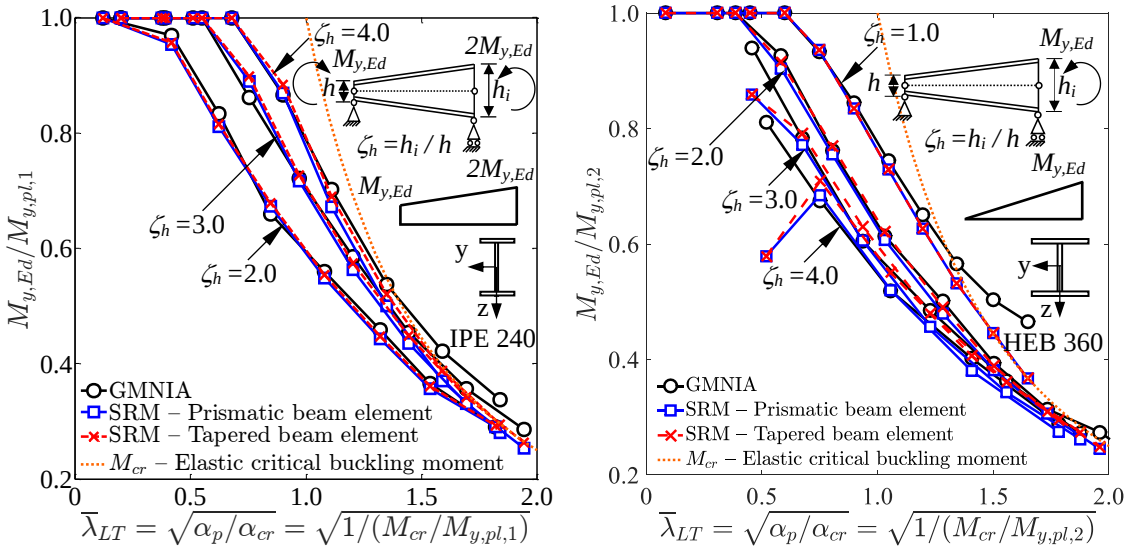


(a) HEB 360

(b) HEM 100

(c) IPE 240

Figure 8: Accuracy of the proposed stiffness reduction method (SRM) in comparison to shell finite element GMNIA and Eurocode 3 [1] for tapered beams under uniform bending with different section shapes and slendernesses



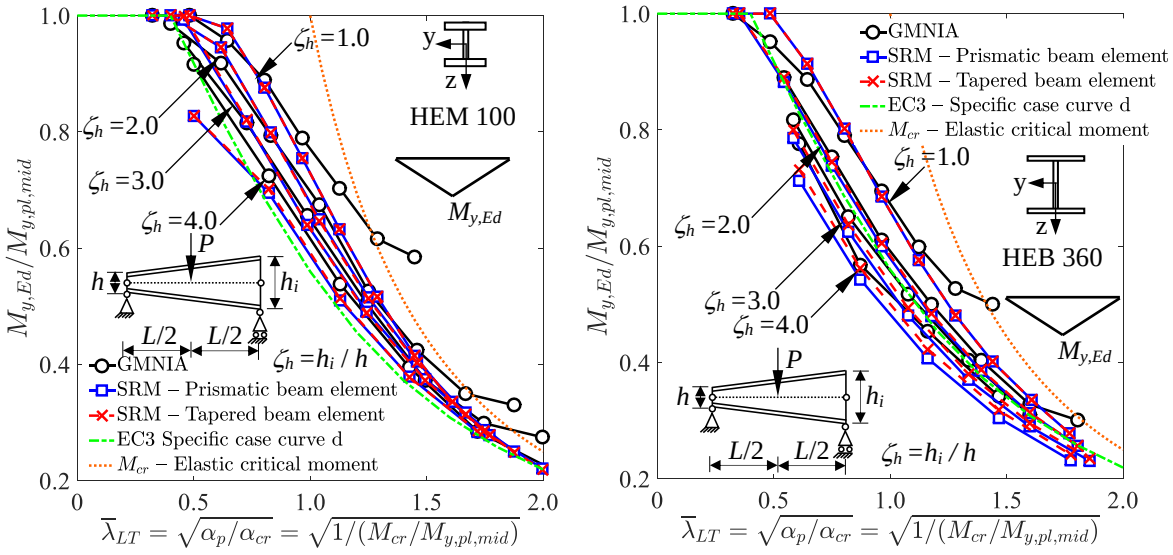
(a) IPE 240 $\mu = 0.5$

(b) HEB 360 $\mu = 0$

(c) HEB 360 $\mu = -0.5$

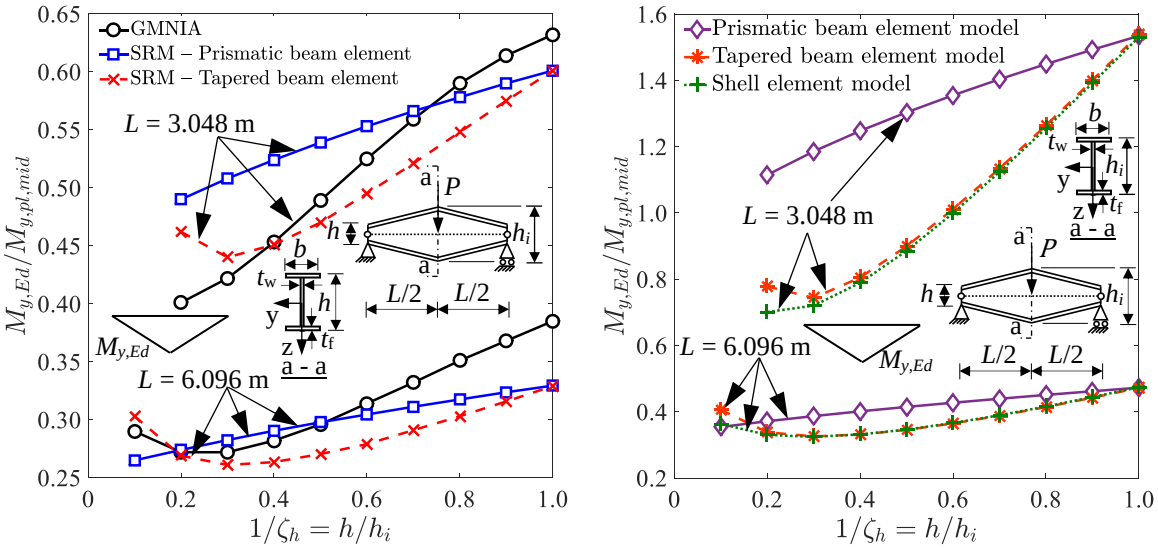
(d) IPE 240 $\mu = -1$

Figure 9: Accuracy of the proposed stiffness reduction method (SRM) in comparison to shell finite element GMNIA for tapered beams under moment gradient with different section shapes and slendernesses



(a) HEM 100 (b) HEB 360

Figure 10: Accuracy of the proposed stiffness reduction method (SRM) in comparison to shell finite element GMNIA and Eurocode 3 [1] for tapered beams subjected to a point load at mid-span with different section shapes and slendernesses



(a) Ultimate strength predictions (b) Elastic critical moment predictions

Figure 11: Accuracy of the stiffness reduction method (SRM) when applied using tapered or prismatic elastic finite elements and accuracy of tapered and prismatic element models in predicting the elastic critical buckling moments of doubly tapered beams ($h_i = 609.6$ mm, $b = 152.4$ mm, $t_w = 9.5$ mm, $t_f = 12.7$ mm)

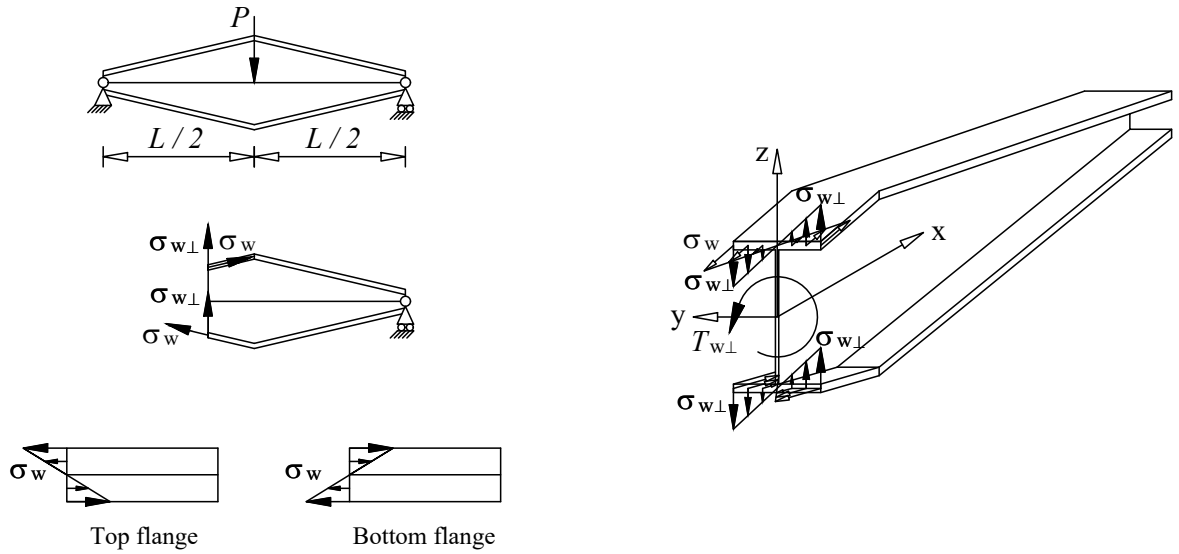


Figure 12: Development of second-order torque $T_{w\perp}$ due to the vertical component $\sigma_{w\perp}$ of the warping normal stresses within flanges σ_w

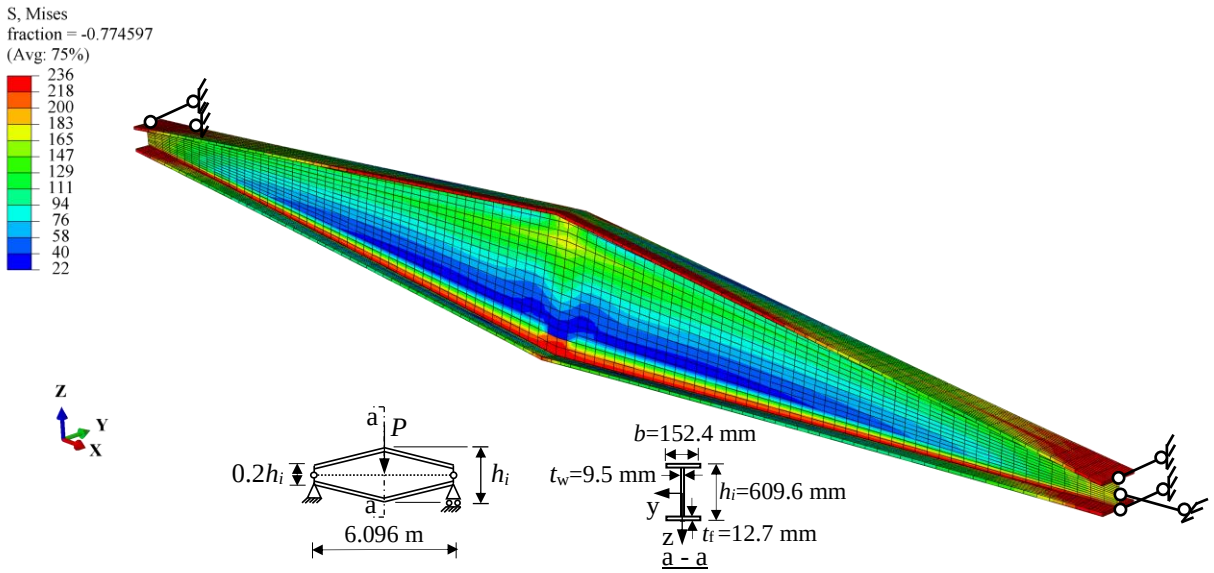


Figure 13: Finite element model of the doubly-tapered Yang and Yau [36] steel beam with $L = 6096$ mm and $1/\zeta_h = 0.2$ after failure

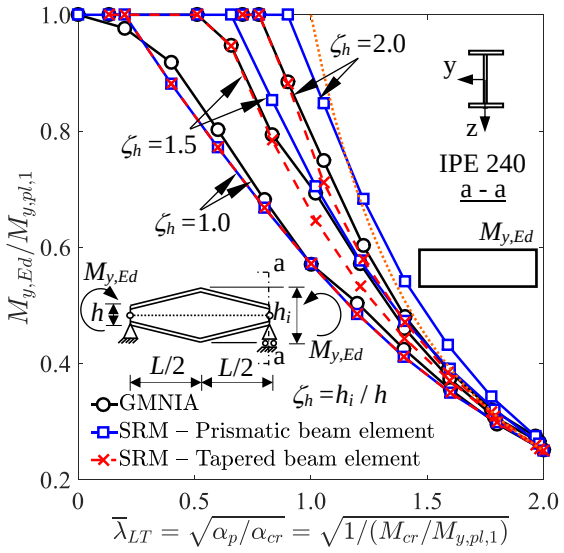


Figure 14: Accuracy of the proposed stiffness reduction method (SRM) in comparison to shell finite element GMNIA for doubly-tapered beams

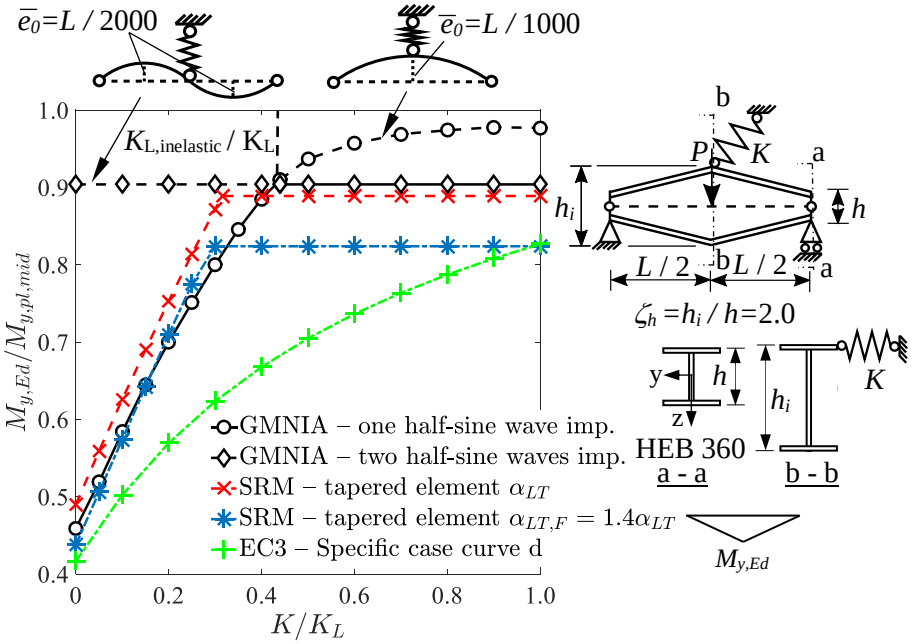
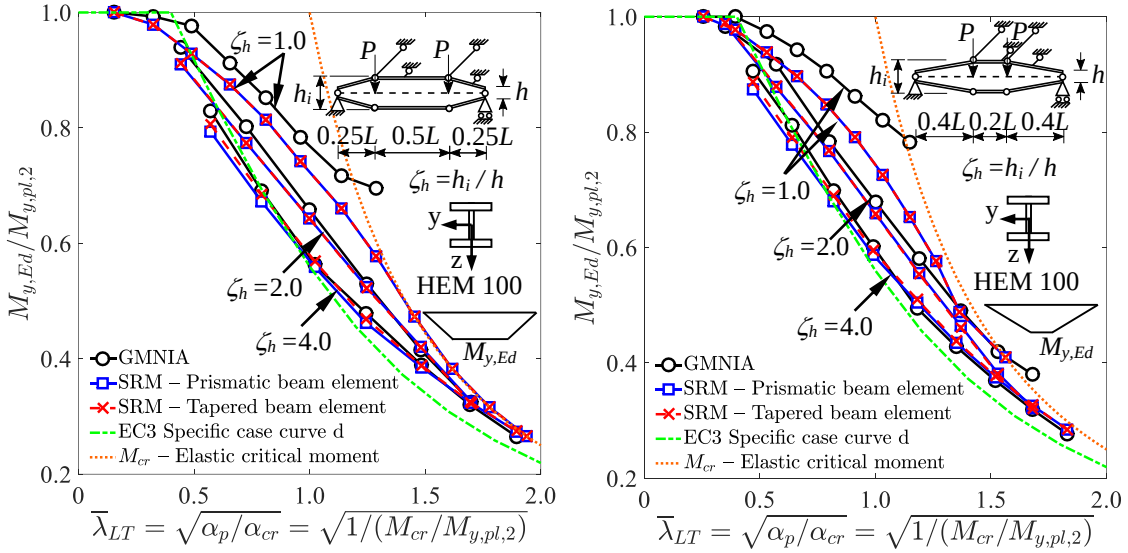
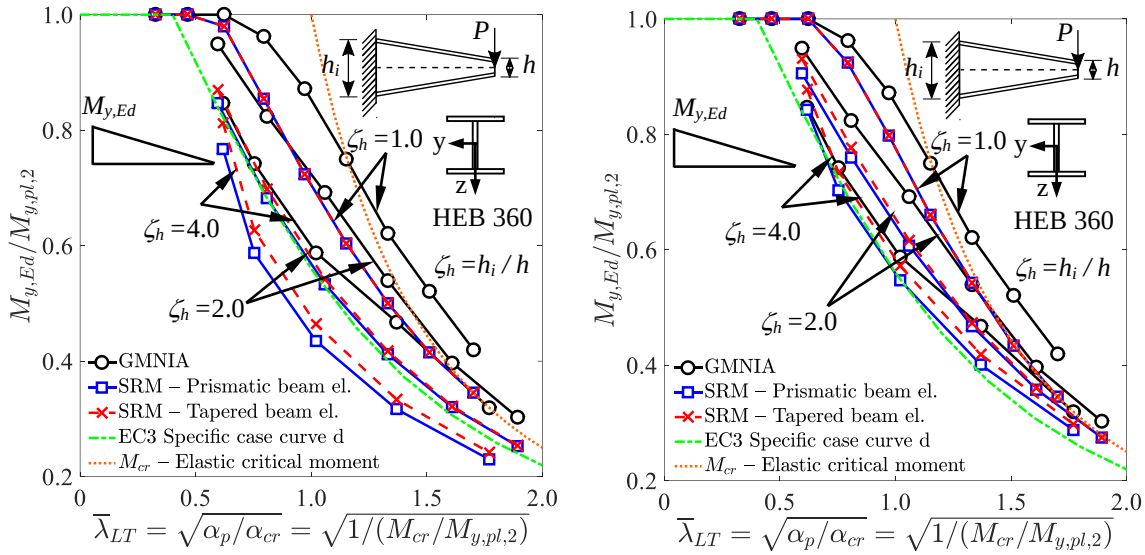


Figure 15: Comparison of ultimate strength predictions determined through the proposed stiffness reduction method (SRM) against shell finite element GMNIA and Eurocode 3 for doubly tapered beams with elastic lateral restraint



(a) $L_o/L_i = 0.5$ (b) $L_o/L_i = 2.0$

Figure 16: Comparison of ultimate strength predictions determined through the proposed stiffness reduction method (SRM) against shell finite element GMNIA and Eurocode 3 for braced tapered beams



(a) SRM with $\alpha_{LT,F} = 1.40\alpha_{LT}$ (b) SRM with α_{LT}

Figure 17: Comparison of ultimate strength predictions determined through the proposed stiffness reduction method (SRM) against shell finite element GMNIA and Eurocode 3 for cantilever tapered beams

Tables captions

Table 1 : Range of cross-section properties considered for the calibration of the Perry-Robertson equation

Table 2 : Values of α_{LT}, β, $\overline{\lambda}_{LT,0}$ and κ proposed in this study and those given in EN 1993-1-1 [1] for the LTB assessment of welded beams

Table 3 : Assessment of accuracy of the proposed Perry-Robertson equation against shell finite element GMNIA results and Eurocode 3 general and specific case LTB equations for welded prismatic beams subjected to uniform bending

Table 4 : Assessment of the proposed stiffness reduction method in comparison to Eurocode 3 [1] for web-tapered welded beams under uniform bending with three different cross-section shapes (i.e. IPE 240, HEM 100, HEB 360) at the shallow end

Table 5 : Assessment of the proposed stiffness reduction method for web-tapered welded beams in comparison to Eurocode 3 [1] under different end moments and transverse loads with HEB 360, HEM 100 and IPE 240 section shapes at the shallow end

Table 1: Range of cross-section properties considered for the calibration of the Perry-Robertson equation

	h/b	b/t_f	h/t_w
Maximum	3.34	25.0	60.6
Minimum	0.91	5.3	10.0

Table 2: Values of α_{LT}, β, $\overline{\lambda}_{LT,0}$ and κ proposed in this study and those given in EN 1993-1-1 [1] for the LTB assessment of welded beams

	This study		Eurocode 3 specific		Eurocode 3 general	
	$h/b \leq 2.0$	$h/b > 2.0$	$h/b \leq 2.0$	$h/b > 2.0$	$h/b \leq 2.0$	$h/b > 2.0$
α_{LT}	$0.33\sqrt{\frac{W_{el,y}}{W_{el,z}}} \leq 0.95$	$0.33\sqrt{\frac{W_{el,y}}{W_{el,z}}} \leq 0.95$	0.49	0.76	0.49	0.76
β	0.60	0.60	0.75	0.75	1.00	1.00
$\overline{\lambda}_{LT,0}$	0.20	0.20	0.40	0.40	0.20	0.20
κ	see eq. (2) but $\kappa \geq 0.55$		1.00	1.00	1.00	1.00

Table 3: Assessment of accuracy of the proposed Perry-Robertson equation against shell finite element GMNIA results and Eurocode 3 general and specific case LTB equations for welded prismatic beams subjected to uniform bending

	Aspect ratio	N	S_{av}	S_{COV}	S_{max}	S_{min}
Proposed equation			1.00	0.022	1.06	0.96
Eurocode 3 – General case	$h/b \leq 2.0$	86	0.91	0.091	1.03	0.77
Eurocode 3 – Specific case			1.04	0.050	1.16	0.92
Proposed equation			0.98	0.030	1.05	0.93
Eurocode 3 – General case	$h/b > 2.0$	66	0.82	0.127	1.03	0.68
Eurocode 3 – Specific case			0.97	0.086	1.12	0.84

Table 4: Assessment of the proposed stiffness reduction method in comparison to Eurocode 3 [1] for web-tapered welded beams under uniform bending with three different cross-section shapes (i.e. IPE 240, HEM 100, HEB 360) at the shallow end

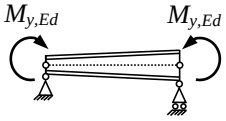
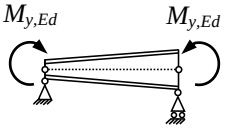
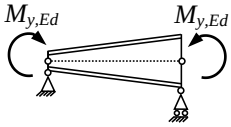
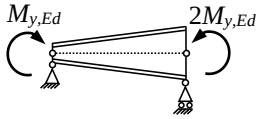
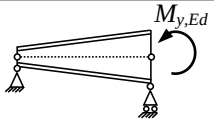
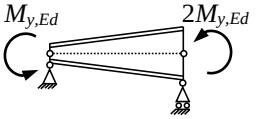
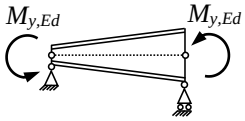
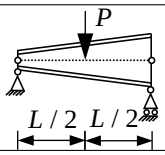
	Loading conditions	ζ_h	N	S_{av}	S_{COV}	S_{max}	S_{min}
SRM – Tapered beam elements		2.0	24	0.99	0.023	1.01	0.90
SRM – Prismatic beam elements				0.98	0.026	1.01	0.89
EC3 – General case curve c				0.79	0.111	1.00	0.62
EC3 – General case curve d				0.72	0.140	1.00	0.53
EC3 – Specific case curve c				0.91	0.073	1.00	0.73
EC3 – Specific case curve d				0.84	0.111	1.00	0.64
SRM – Tapered beam elements		3.0	24	0.98	0.033	1.02	0.89
SRM – Prismatic beam elements				0.98	0.036	1.01	0.86
EC3 – General case curve c				0.78	0.134	1.00	0.58
EC3 – General case curve d				0.71	0.164	1.00	0.51
EC3 – Specific case curve c				0.88	0.091	1.00	0.69
EC3 – Specific case curve d				0.82	0.131	1.00	0.60
SRM – Tapered beam elements		4.0	24	0.97	0.042	1.00	0.85
SRM – Prismatic beam elements				0.97	0.056	1.01	0.81
EC3 – General case curve c				0.77	0.147	1.00	0.60
EC3 – General case curve d				0.71	0.178	1.00	0.52
EC3 – Specific case curve c				0.86	0.106	1.00	0.73
EC3 – Specific case curve d				0.80	0.147	1.00	0.63

Table 5: Assessment of the proposed stiffness reduction method for web-tapered welded beams in comparison to Eurocode 3 [1] under different end moments and transverse loads with HEB 360, HEM 100 and IPE 240 section shapes at the shallow end

	Loading conditions	ζ_h	N	S_{av}	S_{COV}	S_{max}	S_{min}
SRM – Tapered beam el.		2.0, 3.0, 4.0	57	0.99	0.022	1.05	0.93
SRM – Prismatic beam el.				0.98	0.028	1.04	0.91
EC3 – General case curve c				0.82	0.140	1.00	0.59
EC3 – Specific case curve c				0.92	0.096	1.12	0.69
SRM – Tapered beam el.		2.0, 3.0, 4.0	51	1.01	0.025	1.08	0.97
SRM – Prismatic beam el.				0.98	0.032	1.05	0.88
EC3 – General case curve d				0.74	0.126	0.90	0.49
EC3 – Specific case curve d				0.88	0.109	1.01	0.61
SRM – Tapered beam el.		2.0, 3.0, 4.0	68	1.00	0.015	1.06	0.96
SRM – Prismatic beam el.				0.99	0.024	1.04	0.89
EC3 – General case curve c				0.78	0.159	1.00	0.58
EC3 – Specific case curve c				0.88	0.113	1.00	0.69
SRM – Tapered beam el.		2.0, 3.0, 4.0	84	0.99	0.020	1.01	0.91
SRM – Prismatic beam el.				1.00	0.015	1.02	0.93
EC3 – General case curve c				0.78	0.171	1.00	0.59
EC3 – Specific case curve c				0.87	0.121	1.00	0.69
SRM – Tapered beam el.		2.0, 3.0, 4.0	74	0.97	0.044	1.08	0.85
SRM – Prismatic beam el.				0.96	0.051	1.08	0.85
EC3 – General case curve d				0.81	0.123	1.03	0.58
EC3 – Specific case curve d				0.97	0.117	1.23	0.70